INVITED FEATURE ARTICLE

Ecological Applications, 0(0), 2017, pp. 1–23

The role of driving factors in historical and projected carbon dynamics of upland ecosystems in Alaska

Hélène Genet,[1,14] Yujie He,[2] Zhou Lyu,[2] A. David McGuire,[3] Qianlai Zhuang,[2] Joy Clein,[1] David D'Amore,[4] Alec Bennett,[5] Amy Breen,[5] Frances Biles,[4] Eugénie S. Euskirchen,[1] Kristofer Johnson,[6] Tom Kurkowski,[5] Svetlana (Kushch) Schroder,[7] Neal Pastick,[8,9] T. Scott Rupp,[5] Bruce Wylie,[10] Yujin Zhang,[11] Xiaoping Zhou,[12] and Zhiliang Zhu[13]

[1]*Institute of Arctic Biology, University of Alaska Fairbanks, Fairbanks, Alaska 99775 USA*
[2]*Earth, Atmospheric, and Planetary Sciences, Purdue University, West Lafayette, Indiana 47907 USA*
[3]*U.S. Geological Survey, Alaska Cooperative Fish and Wildlife Research Unit, University of Alaska Fairbanks, Fairbanks, Alaska 99775 USA*
[4]*U.S. Department of Agriculture, Forest Service, Pacific Northwest Research Station, Juneau, Alaska 99801 USA*
[5]*Scenarios Network for Alaska and Arctic Planning, International Arctic Research Center, University of Alaska Fairbanks, Fairbanks, Alaska 99775 USA*
[6]*U.S. Department of Agriculture, Forest Service, Northern Research Station, Newtown Square, Pennsylvania 19073 USA*
[7]*School of Environmental and Forest Sciences, University of Washington, Seattle, Washington 98195 USA*
[8]*Stinger Ghaffarian Technologies Inc., contractor to the U.S. Geological Survey, Sioux Falls, South Dakota 57198 USA*
[9]*Department of Forest Resources, University of Minnesota, St. Paul, Minnesota 55108 USA*
[10]*U.S. Geological Survey, The Earth Resources Observation Systems Center, Sioux Falls, South Dakota 57198 USA*
[11]*Chinese Academy of Sciences, Beijing,, China*
[12]*U.S. Department of Agriculture, Forest Service, Pacific Northwest Research Station, Portland, Oregon 97208 USA*
[13]*U.S. Geological Survey, Reston, Virginia 12201 USA*

Abstract. It is important to understand how upland ecosystems of Alaska, which are estimated to occupy 84% of the state (i.e., 1,237,774 km^2), are influencing and will influence statewide carbon (C) dynamics in the face of ongoing climate change. We coupled fire disturbance and biogeochemical models to assess the relative effects of changing atmospheric carbon dioxide (CO_2), climate, logging and fire regimes on the historical and future C balance of upland ecosystems for the four main Landscape Conservation Cooperatives (LCCs) of Alaska. At the end of the historical period (1950–2009) of our analysis, we estimate that upland ecosystems of Alaska store ~50 Pg C (with ~90% of the C in soils), and gained 3.26 Tg C/yr. Three of the LCCs had gains in total ecosystem C storage, while the Northwest Boreal LCC lost C (−6.01 Tg C/yr) because of increases in fire activity. Carbon exports from logging affected only the North Pacific LCC and represented less than 1% of the state's net primary production (NPP). The analysis for the future time period (2010–2099) consisted of six simulations driven by climate outputs from two climate models for three emission scenarios. Across the climate scenarios, total ecosystem C storage increased between 19.5 and 66.3 Tg C/yr, which represents 3.4% to 11.7% increase in Alaska upland's storage. We conducted additional simulations to attribute these responses to environmental changes. This analysis showed that atmospheric CO_2 fertilization was the main driver of ecosystem C balance. By comparing future simulations with constant and with increasing atmospheric CO_2, we estimated that the sensitivity of NPP was 4.8% per 100 ppmv, but NPP becomes less sensitive to CO_2 increase throughout the 21st century. Overall, our analyses suggest that the decreasing CO_2 sensitivity of NPP and the increasing sensitivity of heterotrophic respiration to air temperature, in addition to the increase in C loss from wildfires weakens the C sink from upland ecosystems of Alaska and will ultimately lead to a source of CO_2 to the atmosphere beyond 2100. Therefore, we conclude that the increasing regional C sink we estimate for the 21st century will most likely be transitional.

Key words: Alaska carbon cycle; atmospheric CO_2; carbon balance; climate change; fire; logging; permafrost; soil carbon; upland ecosystem; vegetation productivity.

Manuscript received 6 April 2017; revised 26 July 2017; accepted 25 August 2017. Corresponding Editor: Yude Pan.
Editors' Note: Papers in Invited Features are published individually and are linked online in a virtual table of contents on the journal website.
[14] E-mail: hgenet@alaska.edu

Introduction

The design of efficient policies to mitigate climate change relies on robust predictions of how the carbon (C) balance of terrestrial ecosystems will respond to different pathways of climate change. Because of the large amount of C stored in northern high latitude ecosystems (Schuur et al. 2015), pathways of climate change could be altered by responses of C balance in this region (McGuire et al. 2012). Recent estimate of C stored in permafrost soils (0–3 m) of Arctic and sub-Arctic regions are 1,035 Pg C (±150 Pg C 95% confidence interval; Michaelson et al. 2013, Hugelius et al. 2013, 2014). Because of polar amplification, the rate of warming in the Arctic has been 1.6 times higher than the rate in lower latitudes between 1875 and 2008 (Bekryaev et al. 2010). Climate warming is altering a range of biological and physical processes, including those related to permafrost dynamics and hydrology (Romanovsky et al. 2010, Liljedahl et al. 2016), vegetation composition and productivity (Stow et al. 2004, Beck and Goetz 2011, Myers-Smith et al. 2011) and disturbance regimes such as wildfire (Kasischke and Turetsky 2006, De Groot et al. 2013) and thermokarst (Jorgenson et al. 2001, Lara et al. 2016, Nitze and Grosse 2016). These changes may trigger profound transitions in ecosystem trajectories (Hinzman et al. 2013) that will affect C sequestration and C dynamics at local and regional scales.

Increases in vegetation productivity from rising atmospheric carbon dioxide (CO_2) and air temperature are well documented (Ainsworth and Long 2005, Chapin et al. 2006, Zeng et al. 2011, Bieniek et al. 2015) and can enhance C sequestration in the soil by increasing C input from litterfall (Harden et al. 1992, Yuan et al. 2012). This enhanced C uptake may be partially or wholly offset by C releases to the atmosphere from increases in decomposition and fire emissions in arctic and boreal ecosystems (Hayes et al. 2011). Permafrost thaw driven by climate warming exposes deep soil C to warmer temperatures that can increase decomposition, and ultimately release soil organic C (SOC) to the atmosphere in the form of CO_2 or methane (CH_4), depending on the local drainage conditions (Harden et al. 2006, 2012a,b, Schuur et al. 2008, Hugelius et al. 2013). Additionally, increases in air temperature may lead to an increase in fire frequency and severity (Kasischke et al. 2002, Balshi et al. 2009) that could cause further warming through (1) large pyrogenic C releases to the atmosphere (Turetsky et al. 2011, Genet et al. 2013), (2) decreasing photosynthetic activity from fire-killed vegetation (Goetz et al. 2007), and (3) further thawing of the permafrost through combustion of the insulating organic layer (Jafarov et al. 2013, Johnson et al. 2013, Jones et al. 2015). A recent synthesis has estimated that between 130 and 160 Pg C could be released from soils of the northern permafrost region to the atmosphere during the 21st century under the current warming trajectory given no changes in productivity (Schuur et al. 2015). In addition, it has been estimated that C emissions from wildfire could increase fourfold compared to historical emissions (Abbott et al. 2016). Finally, commercial timber harvest in boreal and coastal forests may impact regional C balance by exporting significant C stocks out of terrestrial ecosystems, and affecting stand age distribution (Cole et al. 2010).

The state of Alaska contains ~7% of the global tundra biome extent (CAVM Team 2003), ~4% of the boreal forest biome extent (Whittaker 1975), and ~5% of the extent of permafrost regions (Brown et al. 1998). Alaska also experiences substantial fire activity (Kasischke et al. 2010), and a large proportion of its landscape is underlain by permafrost vulnerable to significant thaw over the 21st century (Pastick et al. 2017), which would expose previously protected C stocks to decomposition under projected climate change (Turetsky et al. 2011, Hayes et al. 2014). However, spatial and temporal dynamics of fire and thawing permafrost are shaped by landform and drainage conditions. In Alaska, uplands are estimated to occupy 84% of the landscape (Pastick et al. 2017). Compared to lowlands (i.e., wetlands and peatlands), uplands are characterized by better drainage conditions with aerobic soils that promote relatively high rates of decomposition that primarily produce CO_2 (Schuur et al. 2008). Methanogenesis is limited in well-drained soils and CH_4 production can be offset by methanotrophy (Whalen and Reeburgh 1990). Low moisture content and more flammable fuel load are associated with higher frequency of wildfire in well drained uplands compared to poorly drained lowlands (Turetsky et al. 2011, Genet et al. 2013). Additionally, shallow and dry organic layer and frequent wildfire contribute to a lower resilience of permafrost to climate change compared to poorly drained lowlands with lower fire frequency (Jafarov et al. 2013, Johnson et al. 2013). Finally, commercial timber harvest in Alaska occurs mainly in upland maritime forests of southeastern coastal Alaska (i.e., western hemlock [*Tsuga heterophylla* (Raf.) Sarg.] and Sitka spruce [*Picea sitchensis* (Bong.) Carrière] forests). On the other hand, more rapid nutrient cycling and deep rooting occur in well-drained upland ecosystems, which are expected to lead to higher vegetation productivity than lowland ecosystems (Bhatti et al. 2010). Because processes affecting C balance have different sensitivities to climate change, it is important to explicitly separate uplands from lowlands in regional assessments of C dynamics to climate change. This study is focused on C dynamics in uplands of Alaska. Lowland C dynamics of Alaska are the focus of a separate paper in this invited feature (Lyu et al. 2016).

The main goal of this study is to provide an assessment of the historical and future trajectory of C dynamics in upland ecosystems of Alaska and to diagnose the mechanisms responsible for these dynamics. To achieve this goal, we applied a modeling framework that has been designed and calibrated to represent major vegetation communities of upland ecosystems in arctic, boreal and maritime regions of Alaska. We made use of recent

geospatial data to characterize landscape heterogeneity (Pastick et al., this feature). Specifically, this study assesses the C balance of upland ecosystems in Alaska from 1950 through 2099 in the four main Landscape Conservation Cooperative (LCC) regions of Alaska: (1) Arctic LCC, (2) Western Alaska LCC, (3) Northwest Boreal LCC, and (4) North Pacific LCC (Fig. 1). The Landscape Conservation Cooperatives were established by the Department of Interior to support cooperative conservation and sustainable resource management efforts (Landscape Conservation Cooperatives 2012). These regions were chosen as spatial units to stratify this assessment so that the results could inform regional consortia of natural resource agencies, which have been organized into these LCCs. The boundaries of the LCC regions in Alaska closely match the boundaries of the main ecoregions of the state (Nowacki et al. 2001). The Aleutian and Bering Sea Islands LCC was not included in this assessment as it represents about 1.5% of the state area and its contribution to the state carbon balance is expected to be negligible. It is also composed of vegetation communities that are poorly documented and therefore challenging to parameterize. Furthermore, this study includes a comprehensive analysis to evaluate the mechanisms responsible for the projected C dynamics of these four LCCs with respect to the effects of increases in atmospheric CO_2, changes in climate, and changes in fire regime.

Material and Methods

Model framework

Changes in soil and vegetation C pools and fluxes in response to climate change and disturbances were analyzed using a modeling framework that combines a model of wildfire disturbance, the Alaska Frame-Based Ecosystem Code (ALFRESCO; Rupp et al. 2001, 2002, 2007, Johnstone et al. 2011, Mann et al. 2012, Gustine et al. 2014), and two process-based ecosystem models that simulate (1) C and nitrogen (N) pools and CO_2 fluxes with the Dynamic Organic Soil version of the Terrestrial Ecosystem Model (DOS-TEM; Yi et al. 2009a, 2010) and (2) CH_4 fluxes using the Methane Dynamics Module of the Terrestrial Ecosystem Model (MDM-TEM; Zhuang et al. 2004). The three models were coupled asynchronously, in which the time series of fire occurrence simulated by ALFRESCO were used to force DOS-TEM. Monthly NPP and leaf area index (LAI) simulated by DOS-TEM were used to force MDM-TEM. ALFRESCO is a spatially explicit, stochastic landscape succession model designed and parameterized for Arctic and sub-Arctic regions (detailed description of the model in Pastick et al. [2017]). DOS-TEM is a process-based biogeochemical model that estimates soil and vegetation thermal and hydrological regimes, permafrost dynamics and carbon and nitrogen fluxes between soil, vegetation, and the atmosphere, and carbon and nitrogen pools in the soil and the vegetation (Yi et al. 2009a,b, 2010). MDM-TEM is a process-based biogeochemical model that estimates the net flux of CH_4 between soils and the atmosphere based on the rate of CH_4 production and oxidation within the soil profile, and the transport of CH_4 from the soil to the atmosphere (detailed description of the model in Lyu et al. 2016).

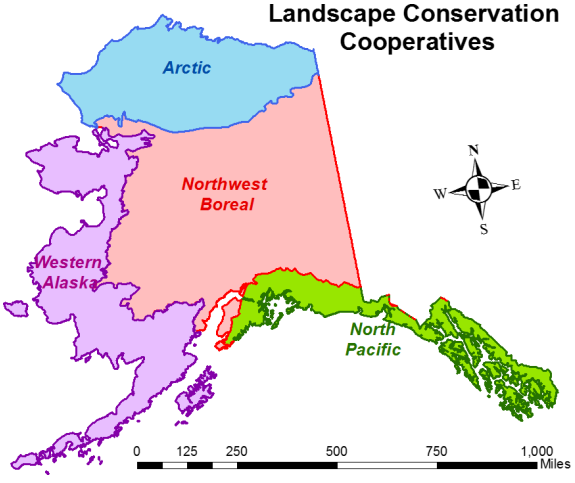

Fig. 1. The four main Landscape Conservation Cooperatives (LCC) in Alaska, USA. 1 mile = 1.6 km.

DOS-TEM description: A process-based ecosystem model

DOS-TEM is composed of four modules: an environmental module, an ecological module, a disturbance module, and a dynamic organic soil module. The environmental module computes dynamics of biophysical processes in the soil and the atmosphere, driven by climate and soil texture input data, leaf area index from the ecological module, and soil structure from the dynamic organic soil module. Soil temperature and moisture conditions are calculated for multiple layers within various soil horizons, including moss, fibric, and humic organic horizons, and mineral horizons (Yi et al. 2009b). A stable snow/soil thermal model integrated into the environmental module uses the Two-Directional Stefan Algorithm (Woo et al. 2004) to simulate the positions of the freeze–thaw front and active-layer thickness (Yi et al. 2006, 2009b). The active layer thickness is the seasonal maximum of thaw depth. The temperature of soil layers above first freezing/thawing front and below the last freezing/thawing front is updated separately by solving finite difference equations. The environmental module provides information regarding the atmospheric and soil environment to the ecological module and the disturbance module. The ecological module simulates C and N dynamics among the atmosphere, the vegetation, and the soil. C and N dynamics are driven by climate input data, information on soil and atmospheric environments from the

environmental module, information on soil structure provided by the dynamic organic soil module, and information on timing and severity of wildfire or forest harvest provided by the disturbance module. DOS-TEM simulates the dynamics of three different soil C horizons (the fibrous, amorphous, and mineral soil horizons), and C and N dynamics in the aboveground and belowground compartments of the vegetation. The C from litterfall is divided into aboveground and belowground litterfall. Aboveground litterfall is assigned only to the first layer of the fibrous horizon, while belowground litterfall is assigned to different layers of the three soil horizons based on the fractional distribution of fine roots with depth. The dynamic organic soil module calculates the thickness of the fibric and sapric/humic organic horizons after soil C pools are altered by ecological processes (litterfall, decomposition, and burial) and fire disturbance. The estimation of organic horizon thickness is computed from soil C content using relationships that link soil organic C content and soil organic thickness (i.e., pedotransfer functions; Yi et al. 2009a). These relationships have been developed for fibric, sapric/humic, and mineral horizons for every vegetation type, based on data from the soil C network database for Alaska (Johnson et al. 2011). Finally, the disturbance module simulates how forest harvest and wildfire affects stand age distribution C and N pools of the vegetation and the soil. For wildfire, the module computes combustion emissions to the atmosphere, the fate of uncombusted C and N pools, and the flux of N from the atmosphere to the soil via biological N fixation in the years following fire. The rates of combustion of the organic layer and the mortality rate in the vegetation depend on fire severity. In boreal forest, fire severity is determined using input data on topography, drainage, and vegetation, as well as soil (moisture and temperature) and atmospheric (evapotranspiration) environmental data from the environmental module (Genet et al. 2013). In tundra, the rates of combustion and vegetation mortality are based on those estimated from the 2007 Anaktuvuk River Fire (Mack et al. 2011). Methane emissions from fire were estimated a posteriori by applying an emission factor as estimated by French et al. (2002) to the fire emissions simulated by DOS-TEM. The effects of forest harvest disturbance on C and N balances are also included in the disturbance module. Commercial timber harvest by clear-cutting has been widespread in southeastern Alaska since the early 1950s (Alaback 1982, Cole et al. 2010). We developed a harvesting function with the assumption that 95% of the aboveground vegetation biomass within a logged stand is harvested (Deal and Tappeiner 2002). Among the residual biomass, 4% was considered dead and 1% alive to allow post-harvest recruitment. As a consequence, 99% of the root vegetation biomass was considered dead and transferred to the soil organic matter pool.

Regional applications of versions of TEM that lead to DOS-TEM in northern high latitudes have investigated how biogeochemical dynamics of terrestrial ecosystems are affected at seasonal to century scales by processes like permafrost thaw and soil thermal dynamics (Zhuang et al. 2002, 2003, Euskirchen et al. 2006), snow cover (Euskirchen et al. 2006, 2007), and warming and fire disturbance (Balshi et al. 2007, Sitch et al. 2007).

DOS-TEM parameterization and validation

Rate-limiting parameters of the model were calibrated for eight main upland land-cover types in Alaska: three types of tundra (graminoid, shrub, heath), three types of boreal upland forest (black spruce [*Picea mariana* (Mill.) Britton, Sterns & Poggenb.], white spruce [*Picea glauca* (Moench) Voss], and deciduous forest), and two types of upland maritime communities (upland Maritime forest and alder shrubland). A detailed description of these land-cover types is available in Pastick et al. (2017).

For each upland land cover type, the rate-limiting parameters of DOS-TEM were calibrated to target values of C and N pools and fluxes representative of mature ecosystems (Clein et al. 2002, see list in target variables in Appendix S1). The calibration of these parameters is an effective means of dealing with temporal scaling issues in ecosystem models (Rastetter et al. 1992). For boreal forest communities, an existing set of target values for vegetation and soil C and N pools and fluxes was assembled using data collected in the Bonanza Creek Long Term Ecological Research program (LTER; Yuan et al. 2012), updated with data from the most recent version of the Bonanza Creek LTER database. For the tundra communities, we used data collected near the Toolik Field Station as part of the Arctic LTER program (Shaver and Chapin 1991, Van Wijk et al. 2003, Sullivan et al. 2007, Euskirchen et al. 2012, Gough et al. 2012, Sistla et al. 2013). Finally, for the maritime upland forest, we used data collected from a long-term C flux study in the North American Carbon Program (D'Amore et al. 2012). The target values for maritime alder shrubland were assembled from Binkley (1982). The target values used for all of these calibrations are listed in Appendix S1.

The DOS-TEM parameterizations were validated using soil and vegetation biomass data derived from field observations independent of the data used for model calibration. The validation analysis for DOS-TEM is presented in Genet et al. (2016). The National Soil Carbon Network database for Alaska (Johnson et al. 2011) was used to validate DOS-TEM estimates of soil C pools. To compare similar estimates from the model and observations, only deep profiles were selected from the database, i.e., profiles with a description of the entire organic horizons and 90 to 110 cm thick mineral horizon below the organic horizons. Estimates of vegetation C pools for tundra land-cover types were compared with observations recorded in the data catalog of the Arctic LTER at Toolik Field Station. For boreal forest land-cover types, vegetation C pools simulated by DOS-TEM were compared with estimates from forest inventories conducted by the Cooperative Alaska Forest Inventory Program (Malone

et al. 2009). The forest inventory only provided estimates of aboveground biomass. Aboveground biomass was converted to total biomass by using a ratio of aboveground vs. total biomass of 0.8 in forest (Ruess et al. 1996) and 0.6 in tundra land-cover types (Gough et al. 2012). The content of C in biomass was estimated at 50%. Finally, for the land-cover types of southeastern coastal Alaska (that is, the North Pacific LCC maritime upland forest and alder shrubland), model validation was not possible as no additional independent data were available in this region (the plot coordinates of the Forest Inventory of Alaska not being available, site specific comparisons were not possible). For these land-cover types, we compared the model simulations with observed data on the same sites that were used for model parameterization. No significant differences were observed between modeled and observed contemporary vegetation and soil C stocks (P values of 0.340 and 0.085, respectively). Additionally, DOS-TEM simulations successfully reproduced differences between land-cover types.

Model application

The distribution of uplands in Alaska was assessed from a new, 1-km resolution, wetland map for Alaska identifying upland, fen, bogs, and open waters. The wetland map was developed using the Alaska National Wetlands Inventory as a reference data set (*available online*).[15] This map is described in detail by Pastick et al. (2017). Uplands in Alaska are estimated to cover 1,237,775 km^2, which represents about 84% of the area of the state. The upland vegetation communities were identified using a baseline land cover map derived from the 2005 map from the North America Land Cover Monitoring System (Natural Resources Canada/Canadian Center for Remote Sensing [NRCan/CCRS] et al. 2005).

Simulations were conducted across Alaska at a 1-km resolution from 1950 through 2099. DOS-TEM is driven by annual atmospheric CO_2 concentration, monthly mean air temperature, total precipitation, net incoming shortwave radiation, and vapor pressure. The atmospheric CO_2 and climate projections were aligned with the Intergovernmental Panel on Climate Change's Special Report on Emission Scenarios (IPCC-SRES; Nakicenovic et al. 2000). The assessment was driven by three CO_2 concentration trajectories associated with low-, mid- and high-range CO_2 emission scenarios (A1b, A2, and B1, respectively; Fig. 2a).

Before conducting the transient simulations, a typical spin-up procedure was conducted for each spatial location in which the model was driven by averaged modern forcings for that location, repeated continuously until dynamic equilibrium was achieved (i.e., constant pools and fluxes at that location). The resulting modelled ecosystem state for each spatial location then served as the starting point for the transient simulation during the historical and future periods presented in this study.

To evaluate the effects of historical and projected climate warming, simulations were driven by output from two climate models for each of the three emission scenarios (Fig. 2b, c). Each of the six climate scenarios utilized the same downscaled historical climate data from 1901 through 2009 from the Climatic Research Unit (CRU TS 3.1; Harris et al. 2014). The climate projections were developed for 2010 through 2099 from the outputs of (1) version 3.1-T47 of the Coupled Global Climate Model (CGCM3.1; McFarlane et al. 1992) developed by the Canadian Centre for Climate Modelling and Analysis and (2) version 5 of the European Centre Hamburg Model (ECHAM5; Roeckner et al. 2004) developed by the Max Planck Institute (models *available online*.[16,17] Additional methodological details for the downscaled climate variables can be found in Pastick et al. (2017).

The fire occurrence data set combined (1) historical records from 1950 through 2009 obtained from the Alaska Interagency Coordination Center large fire scar database (Kasischke et al. 2002; database available online)[18] and (2) projected scenarios from ALFRESCO (Pastick et al. 2017). These scenarios represent the anticipated changes in fire frequency in response to climate change, and resulting changes in vegetation composition over time due to fire disturbance and secondary succession (Fig. 2d). ALFRESCO produces an ensemble of simulations (n = 200) for each climate scenario to represent the uncertainty of the response of fire regime to climate. Replicating DOS-TEM simulations across the region for each scenario would have been impractical as these simulations are computationally intensive. Subsequently, for each climate scenario, the fire time series selected to run DOS-TEM simulations were the simulation that best reproduced historical fire records in terms of annual area burned and mean fire size. Topographic information from the National Elevation Dataset of the U.S. Geological Survey at 60-m resolution (NED) was used to calculate fire severity with the algorithm of Genet et al. (2013); NED available online .[19] The topographic descriptors included slope, aspect, and log-transformed flow accumulation.

Historical records of forest harvest area from 1950 through 2009 in southeast and south-central Alaska were compiled from geographic information system data from four different sources: (1) the USDA Forest Service, Tongass National Forest; (2) the Nature Conservancy's past harvest repository; (3) the State of Alaska Department of Natural Resources; and (4) screen digitizing from high-resolution orthophotos of some harvests not included in the previously listed sources. In

[15] http://www.fws.gov/wetlands/Data/State-Downloads.html

[16] https://www.canada.ca/en/environment-climate-change/services/climate-change/centre-modelling-analysis/models/third-generation-coupled-global.html

[17] https://www.mpimet.mpg.de/en/science/models/mpi-esm/

[18] http://fire.ak.blm.gov/

[19] http://ned.usgs.gov/

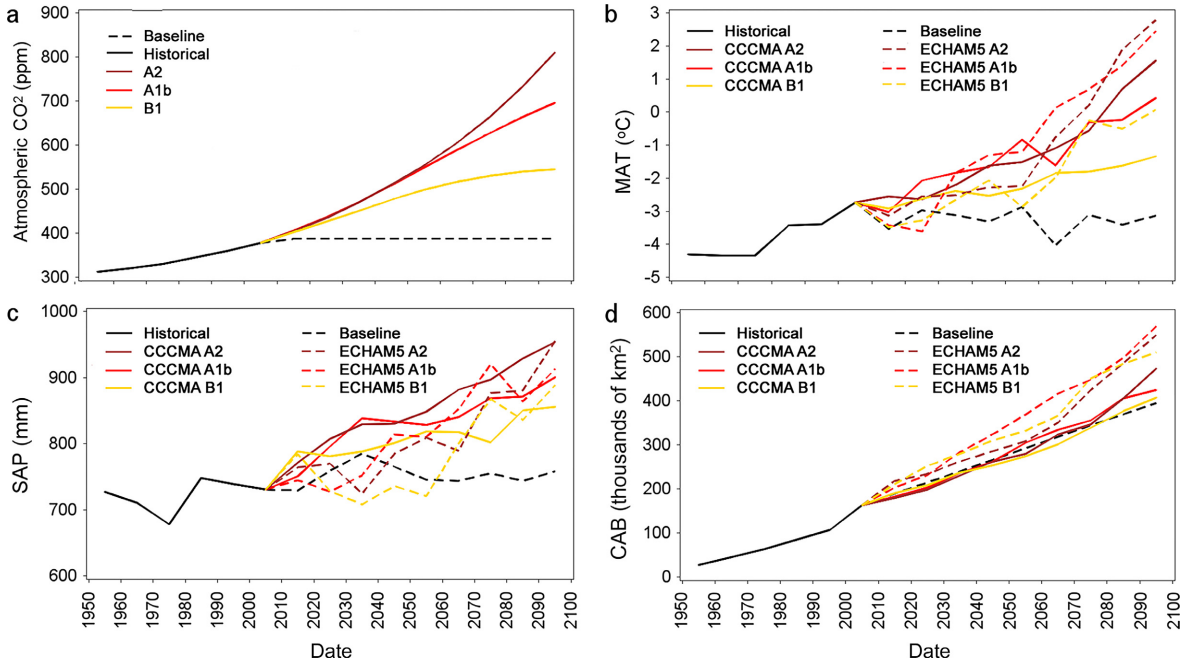

FIG. 2. Decadal averages of (a) atmospheric CO_2, (b) mean annual temperature (MAT), (c) sum of annual precipitation (SAP) and, (d) cumulative area burned (CAB) for the historical period (1950–2009; black solid line) and the projected period (2010–2099) for the two climate models applied to three emission scenarios (gold, orange, and brown lines) and for the baseline (gray dotted line).

addition, the first three sources were edited using high-resolution orthophotos to improve some of the boundary delineations. Second-growth stands from past forest harvest account for about 3.8% of southeast Alaska. We were unable to obtain reliable forest harvest data for areas west of approximately 142.55° W longitude. We used the harvest data to determine where and when forest harvest has taken place. Forest harvest was considered only for the historical period and was not included in the future period, as spatially and temporally explicit projections of forest harvest were not available for the region at the time this assessment was conducted.

Attribution analysis

The relative effect of increasing atmospheric CO_2, climate change and increasing fire regime on ecosystem C balance was analyzed for the projection period (2009–2099), based on model simulations that included various combinations of time series for constant atmospheric CO_2, detrended climate variables, and normalized fire regime. As mentioned in the previous section, the effect of harvest was not included in the attribution analysis as spatially and temporally explicit projections of forest harvest were not available for the region at the time this assessment was conducted. For the constant CO_2 simulation, the atmospheric CO_2 of the baseline simulation was set at the 2009 concentration. The climate time series data were detrended for every 1-km pixel in each variable. A linear regression was fitted to the time series of mean air temperature, precipitation, short-wave incoming radiation, and vapor pressure. The detrended climate variables were then computed (Eq. 1), as a function of the mean value (X_m) of the variable for the last decade of the historical period 2000–2009, and the difference between the current (X_{curr}) and predicted variable (X_{pred})

$$X = \mathrm{Xm} + (\mathrm{Xcurr} - \mathrm{Xpred}). \quad (1)$$

The normalized fire regime data set was generated by using a constant fire return interval (FRI) that was developed from the 1960–1989 fire records (Yuan et al. 2012). This scenario represents a constant fire frequency over time that reflects conditions prior to the significant increase of annual area burned observed in Alaska beginning in the 1990s. For each year, the group of pixels that were burned was randomly selected based on the last time they burned (in other words, the stand age) and the value of the FRI.

To determine the relative effects of rising atmospheric CO_2, changing climate, and fire regime, a set of 10 state-wide simulations was conducted from 2009 to 2099, in addition to the six state-wide projections described above (i.e., CO_2 + climate + fire simulations, see *Model application*). The baseline simulation combined constant atmospheric CO_2, detrended climate, and normalized fire regime. Three simulations combined the three scenarios of CO_2 emissions (B1, A1b, and A2) with detrended climate and normalized fire regime (CO_2

simulations). Finally, six simulations were conducted with rising atmospheric CO_2, and the six climate model-scenarios and normalized fire regime (CO_2 + climate simulations). The effect of CO_2 fertilization was estimated by comparing baseline simulations with the CO_2 simulations. The effect of climate change was estimated by comparing decadal averages from the CO_2 simulations with the decadal averages from the CO_2 + climate simulations. Finally, the effect of a changing fire regime was estimated by comparing the CO_2 + climate simulations with the CO_2 + climate + fire simulations.

Assessing ecosystem C balance

Vegetation C stock estimates were derived from the sum of aboveground and belowground living biomass. Soil C pools were composed of C stored in the dead woody debris fallen to the ground, moss and litter, organic layers and mineral layers. Historical changes in soil and vegetation C pools were evaluated by quantifying cumulative changes from the estimate of the respective C pool at the end of 1949. Projected changes in soil and vegetation C pools were evaluated by quantifying cumulative changes from the estimate of the respective C pool at the end of 2009.

The net ecosystem carbon balance (NECB) is the difference between total C inputs and total C outputs to the ecosystem (Chapin et al. 2006). NECB is the sum of all C fluxes coming in and out of the ecosystems, through gaseous and nongaseous, dissolved and non-dissolved exchanges with the atmosphere and the hydrologic network. In the present study, the C exchange between terrestrial and aquatic ecosystems are not considered. In terrestrial ecosystems, NECB (Eq. 2) is the sum of net primary productivity (NPP) and net biogenic methane flux ($BioCH_4$) minus heterotrophic respiration (HR), fire emissions (Fire), and forest harvest exports (Harvest, for the historical simulation only)

$$\mathrm{NECB} = \mathrm{NPP} + \mathrm{BioCH_4} - \mathrm{HR} - \mathrm{Fire} - \mathrm{Harvest}. \quad (2)$$

NPP results from C assimilation from vegetation photosynthesis minus the respiration of the primary producers (autotrophic respiration). The activity of soil methanotrophs dominates the methane cycle in uplands. For this reason, $BioCH_4$ is a positive net flux from the atmosphere into upland ecosystems. HR results from the decomposition of unfrozen SOC. Fire emissions include C from CO_2, CH_4, and carbon monoxide (CO) emissions. Forest harvest quantifies the amount of vegetation C that is exported out of the terrestrial ecosystem to the wood products sector. Positive NECB indicates a gain of C to the ecosystem from the atmosphere (C sink), and negative NECB indicates a loss of C from the ecosystem to the atmosphere and harvested wood product pool (C source). Uncertainty of NECB associated with the climate scenarios was quantified by the standard deviation among the six tested scenarios of mean NECB for the last decade of the 21st century (i.e., CO_2 + climate + fire simulations).

Statistical analysis of the environmental drivers of ecosystem C balance

The annual environmental and biogeochemical variables at the native 1-km resolution were spatially and temporally autocorrelated. To minimize autocorrelation, which would result in underestimation of the true variance in ordinary least square regression techniques, the experimental unit for the environmental and biogeochemical variables consisted of decadal averages for each of the LCC regions. The effect of CO_2 fertilization on NPP was evaluated by examining the relationship between the relative change in NPP and the change in atmospheric CO_2. The effect of climate change on NPP and HR was evaluated by examining the relationship between the relative change in the respective C flux and the changes in annual mean air temperature, annual sum of precipitation, annual mean net incoming radiation and annual mean vapor pressure. The effect of fire regime was evaluated by examining the relationships between the relative change in area burned and the relative changes in NPP, HR, and NECB as well as between the relative change in area burned and the absolute change in fire emissions. Finally, the environmental drivers of HR were evaluated by comparing decadal averages of HR with decadal averages of vegetation litterfall, soil temperature and organic horizon thickness.

To conduct the comparison among LCC regions with different ranges of NPP and to facilitate the comparison of our attribution analysis with existing literature, changes in NPP and HR (Eq. 3) were estimated as relative changes

$$\Delta \mathrm{Xi,j} = [\mathrm{Xi,j\ (scenario)} - \mathrm{Xi,j\ (baseline)}]/\mathrm{Xi,j\ (baseline)} \quad (3)$$

where ΔXi,j is the relative change of the C flux X for the decade i and the LCC region j, Xi,j (scenario) and Xi,j (baseline) are the value of that C flux X for the scenario run and the baseline run, respectively, for the decade i and the LCC region j. The changes in fire emissions were not computed relatively as baseline fire emission could equal zero in LCC regions with low fire activity.

In contrast, the range of changes in environmental drivers was in general similar among LCC regions, so the change in atmospheric CO_2 and climate variables (Eq. 4) were computed as the simple difference between the scenario and the baseline run

$$\Delta \mathrm{Xi,j} = \mathrm{Xi,j\ (scenario)} - \mathrm{Xi,j\ (baseline)}. \quad (4)$$

The relationship between changes in C fluxes and changes in environmental drivers were evaluated using ordinary least square regression. The differences between LCC regions were evaluated using Analysis of Variance.

All analyses were performed using the SAS statistical package (SAS 9.4; SAS Institute, Cary, North Carolina, USA). The assumptions of normality and homoscedasticity were verified by examining residual plots. Effects were considered significant at the 0.05 level. Averages of C stocks and fluxes are accompanied with the estimated standard deviation from annual variations (SD).

Results

Historical C dynamics of upland ecosystems in Alaska from 1950 through 2009

Our simulations indicate that C storage of upland ecosystems in Alaska increased by 0.20 Pg C from 51.21 Pg C at the end of 1949 to 51.41 Pg C at the end of 2009 (Table 1). The statewide gain of 3.26 Tg C/yr occurred because C gains from NPP and incidentally biogenic CH_4 uptake were greater than losses from HR, logging, and fire (Table 2). Soils were estimated to have increased by 0.23 Pg C across the time period to 47.13 Pg C at the end of 2009, while vegetation was estimated to have lost 0.03 Pg C across the time period to 4.28 Pg C at the end of 2009 (Table 1).

There was variability in the estimated changes in C storage among the LCC regions during the historical period, with gains in the Arctic (0.19 Pg C), North Pacific (0.16 Pg C), and Western Alaska LCCs (0.21 Pg C), and losses in the Northwest Boreal LCC (−0.36 Pg C). The gains in the former three LCCs were dominated by gains in soil C (Table 1), while the losses in the Northwest Boreal LCC were one-third from vegetation C (−0.12 Pg C) and two-thirds from soil C (−0.24 Pg C). Gains in the Arctic and North Pacific LCCs occurred largely because increases in NPP (annual gains are 0.132 and 0.054 Tg C/yr respectively; $P < 0.001$ for both LCCs) were greater than increases in HR (annual gains are 0.092 and 0.033 Tg C/yr respectively; $P = 0.003$ and 0.370, respectively). In the Northwest Boreal LCC, NPP also significantly increased over time (annual gains = 0.066 Tg C/yr; $P = 0.024$), while HR did not change significantly ($P = 0.251$). But this increase in NPP was not enough to compensate for increases in fire emissions during this time period (annual gains = 0.244 Tg C/yr; $P = 0.048$). In the Western Alaska LCC, the increase in NPP (annual gains = 0.083 Tg C/yr; $P = 0.042$) was greater, but non-significant ($P = 0.339$), than the combined increase in HR and fire emissions. Statewide, the C loss during an individual large fire year like 1957, 1969, 2004, 2005, and 2009 was approximately equivalent to the C accumulated during a decade (Fig. 3).

Projected C dynamics of upland ecosystems in Alaska from 2010 through 2099

From 2010 through 2099, total C storage in upland ecosystems of Alaska is estimated to increase by 1.77 (ECHAM5 B1) to 6.03 (CCCMA A1b) Pg C across the

Table 1. Mean annual change in vegetation, soil, and total C stocks for the historical period (from end of 1949 through end of 2009) and vegetation, soil, and total C stocks at the end of 2009 and in each Landscape Conservation Cooperative region and statewide in Alaska, USA.

		Vegetation C		Soil C		Total C	
LCC	Upland area (km^2)	Annual change (Tg C/yr)	Pool in 2009 (Tg C)	Annual change (Tg C/yr)	Pool in 2009 (Tg C)	Annual change (Tg C/yr)	Pool in 2009 (Tg C)
Arctic	261,481	0.82	352.85	2.34	1,0873.11	3.16	1,1225.96
Northwest Boreal	498,879	−2.05	1,738.24	−3.96	1,3631.39	−6.01	1,5369.64
North Pacific	150,087	0.03	11,22.65	2.64	4,811.54	2.67	5,934.19
Western Alaska	327,327	0.65	1,061.59	2.80	17,817.35	3.44	18,878.93
Statewide	1,237,774	−0.56	4,275.32	3.82	47,133.40	3.26	51,408.72

Table 2. Mean C fluxes into and out of Alaska upland ecosystems for the historical period (1950–2009) in each Landscape Conservation Cooperative region and statewide.

LCC	NPP (Tg C/yr)	HR (Tg C/yr)	Logging (Tg C/yr)	Biogenic methane uptake (Gg C/yr)	Pyrogenic methane emissions (Tg C/yr)	Fire $CO + CO_2$ emissions (Tg C/yr)	NECB (Tg C/yr)
Arctic	28.68 (2.89)	−24.80 (0.20)	NA	0.76 (1.47)	$\ll -0.01$	−0.71 (1.81)	3.16 (2.19)
Northwest Boreal	93.14 (3.95)	−86.57 (2.42)	NA	3.24 (7.49)	−0.04 (0.33)	−12.53 (21.91)	−6.01 (25.07)
North Pacific	24.23 (1.68)	−19.96 (0.00)	−1.60 (2.59)	1.59 (4.10)	$\ll -0.01$	$\ll -0.01$	2.67 (4.78)
Western Alaska	58.73 (3.68)	−48.90 (1.18)	NA	1.12 (3.34)	−0.02 (0.39)	−6.37 (10.69)	3.44 (11.16)
Statewide	204.78 (9.82)	−180.23 (20.35)	−1.60 (2.59)	6.71 (5.73)	−0.06 (0.09)	−19.62 (27.31)	3.26 (30.21)

Notes: Numbers in parenthesis indicate inter-annual standard deviation. Positive numbers indicate uptake of C into upland ecosystems and negative numbers indicates losses of C. NA indicates not applicable. NPP, net primary production; HR, heterotrophic respiration; NECB, net ecosystem carbon balance.

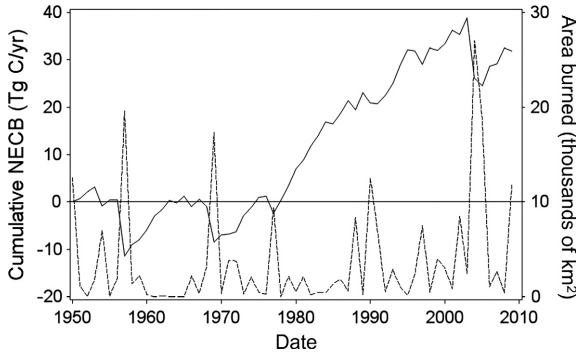

FIG. 3. Statewide cumulative annual Net Ecosystem Carbon Balance (NECB; solid line) and total annual area burned (dotted line), from 1950 to 2009, for upland ecosystems in Alaska.

climate scenarios we analyzed (Table 3), which represents 3.4–11.7% increase in total C storage. Most of the increase in C storage was in soils (+1.02 to +5.27 Pg C for ECHAM5 B1 and CCCMA A1b, respectively). Vegetation C is estimated to increase by 0.50 (CCCMA B1) and 1.02 (ECHAM5 A2) Pg C across the climate scenarios we analyzed. Compared to the historical period (Table 2), statewide NPP and fire emissions increased for all scenarios (Table 4). In contrast, HR decreased for all scenarios except for ECHAM5 B1 (Table 4).

Among the LCCs, the highest gains in total C storage were for CCCMA A1b (the same as statewide) except for the Northwest Boreal LCC, where the highest gains were for ECHAM5 A1b (Table 3). The climate scenario that resulted in the smallest gains in total C storage varied among the LCCs, with only the Western Alaska

TABLE 3. Mean annual change in vegetation, soil, and total carbon stocks during the projection period (end of 2009 through end of 2099) and the final vegetation, soil, and total carbon stocks at the end of 2099 in each Landscape Conservation Cooperative region and statewide, for each climate scenario tested.

	Vegetation C		Soil C		Total C	
LCC and scenario	Annual change (Tg C/yr)	Pool in 2099 (Tg C)	Annual change (Tg C/yr)	Pool in 2099 (Tg C)	Annual change (Tg C/yr)	Pool in 2099 (Tg C)
Arctic						
CCCMA A1b	0.88	433.20	6.77	11,489.61	7.66	11,922.81
CCCMA A2	0.72	418.63	4.22	11,257.48	4.95	11,676.11
CCCMA B1	0.68	414.73	1.14	10,976.95	1.82	11,391.67
ECHAM5 A1b	1.26	467.40	2.99	11,145.60	4.25	11,612.99
ECHAM5 A2	1.48	487.17	3.96	11,233.65	5.44	11,720.82
ECHAM5 B1	0.83	428.29	3.55	11,196.54	4.38	11,624.83
Northwest Boreal						
CCCMA A1b	3.01	2,011.83	14.38	14,940.38	17.39	16,952.21
CCCMA A2	2.72	1,985.37	9.29	14,476.75	12.01	16,462.13
CCCMA B1	1.98	1,918.22	4.51	14,041.39	6.48	15,959.61
ECHAM5 A1b	4.00	2,102.53	14.54	14,954.39	18.54	17,056.91
ECHAM5 A2	4.19	2,119.93	5.84	14,163.11	10.04	16,283.04
ECHAM5 B1	3.32	2,040.55	5.65	14,145.22	8.97	16,185.77
North Pacific						
CCCMA A1b	2.49	1,349.53	5.00	5,266.18	7.49	6,615.71
CCCMA A2	2.81	1,378.41	2.02	4,995.77	4.84	6,374.18
CCCMA B1	1.92	1,297.04	3.57	5,136.64	5.49	6,433.67
ECHAM5 A1b	3.05	1,400.43	1.07	4,909.12	4.12	6,309.55
ECHAM5 A2	2.68	1,366.81	0.61	4,867.47	3.30	6,234.27
ECHAM5 B1	2.19	1,322.05	1.43	4,941.34	3.62	6,263.38
Western Alaska						
CCCMA A1b	1.97	1,241.16	31.74	20,705.66	33.71	21,946.82
CCCMA A2	1.80	1,224.98	4.08	18,188.71	5.88	19,413.69
CCCMA B1	0.91	1,144.44	16.07	19,279.43	16.98	20,423.87
ECHAM5 A1b	2.67	1,304.65	17.18	19,381.13	19.86	20,685.78
ECHAM5 A2	2.90	1,325.16	4.91	18,264.30	7.81	19,589.46
ECHAM5 B1	1.91	1,235.74	0.58	17,870.58	2.50	19,106.32
Statewide						
CCCMA A1b	8.36	5,035.71	57.89	52,401.83	66.25	57,437.54
CCCMA A2	8.04	5,007.39	19.62	48,918.71	27.66	53,926.10
CCCMA B1	5.48	4,774.42	25.29	49,434.40	30.77	54,208.82
ECHAM5 A1b	10.99	5,275.01	35.79	50,390.23	46.77	55,665.24
ECHAM5 A2	11.25	5,299.06	15.33	48,528.54	26.58	53,827.60
ECHAM5 B1	8.26	5,026.63	11.21	48,153.67	19.47	53,180.30

TABLE 4. Mean C fluxes into and out of Alaska upland ecosystems for the projection period (2010 through 2099) in each Landscape Conservation Cooperative region and statewide.

LCC and scenario	NPP (Tg C/yr)	HR (Tg C/yr)	Biogenic methane uptake (Gg C/yr)	Pyrogenic methane emissions (Tg C/yr)	Fire $CO + CO_2$ emissions (Tg C/yr)	NECB (Tg C/yr)
Arctic						
CCCMA A1b	35.80 (3.60)	−26.92 (0.19)	0.83 (1.56)	−0.00 (0.13)	−1.22 (1.69)	7.66 (5.15)
CCCMA A2	37.05 (5.66)	−23.62 (1.23)	0.84 (1.65)	−0.03 (0.19)	−8.45 (11.12)	4.95 (6.58)
CCCMA B1	36.71 (4.06)	−33.18 (0.21)	0.83 (1.62)	−0.01 (0.12)	−1.70 (1.92)	1.82 (4.18)
ECHAM5 A1b	43.83 (6.73)	−29.32 (1.41)	0.86 (1.67)	−0.03 (0.25)	−10.22 (12.79)	4.25 (9.47)
ECHAM5 A2	41.19 (7.08)	−24.79 (1.80)	0.86 (1.67)	−0.04 (0.20)	−10.93 (16.31)	5.44 (11.69)
ECHAM5 B1	38.63 (4.56)	−27.41 (1.09)	0.85 (1.67)	−0.02 (0.18)	−6.81 (9.87)	4.38 (11.87)
Northwest Boreal						
CCCMA A1b	97.47 (7.52)	−63.47 (1.63)	3.62 (8.71)	−0.05 (0.67)	−16.55 (14.76)	17.39 (20.36)
CCCMA A2	96.30 (5.99)	−60.64 (2.15)	3.68 (11.77)	−0.08 (0.48)	−23.58 (19.47)	12.01 (12.00)
CCCMA B1	95.12 (4.14)	−66.45 (1.96)	2.94 (7.05)	−0.07 (0.43)	−22.11 (17.73)	6.48 (13.62)
ECHAM5 A1b	106.33 (8.22)	−66.18 (2.00)	3.73 (11.72)	−0.07 (0.63)	−21.54 (18.15)	18.54 (18.79)
ECHAM5 A2	104.15 (8.51)	−73.23 (2.54)	3.76 (9.95)	−0.07 (0.41)	−20.82 (23.00)	10.04 (23.61)
ECHAM5 B1	100.95 (7.12)	−76.48 (2.01)	2.97 (6.94)	−0.05 (0.46)	−15.45 (18.24)	8.97 (16.18)
North Pacific						
CCCMA A1b	28.83 (3.36)	−21.21 (0.03)	1.72 (4.69)	−0.00 (0.11)	−0.13 (0.27)	7.49 (3.62)
CCCMA A2	29.24 (5.22)	−22.39 (0.32)	1.74 (5.76)	−0.01 (0.12)	−2.00 (2.89)	4.84 (6.20)
CCCMA B1	28.02 (2.14)	−22.46 (0.02)	1.71 (4.26)	−0.00 (0.07)	−0.07 (0.15)	5.49 (2.69)
ECHAM5 A1b	33.47 (5.58)	−25.83 (0.56)	1.71 (5.78)	−0.01 (0.13)	−3.50 (5.04)	4.12 (4.92)
ECHAM5 A2	28.68 (3.55)	−23.57 (0.38)	1.72 (5.19)	−0.01 (0.17)	−1.81 (3.41)	3.30 (5.65)
ECHAM5 B1	29.74 (3.30)	−23.61 (0.38)	1.68 (4.24)	−0.01 (0.13)	−2.51 (3.46)	3.62 (4.13)
Western Alaska						
CCCMA A1b	66.77 (6.86)	−28.93 (0.69)	1.33 (3.80)	−0.01 (0.66)	−4.12 (6.27)	33.71 (21.69)
CCCMA A2	67.64 (7.28)	−46.34 (2.13)	1.34 (3.87)	−0.05 (0.44)	−15.37 (19.32)	5.88 (16.11)
CCCMA B1	65.68 (4.26)	−40.51 (1.04)	1.23 (4.10)	−0.03 (0.68)	−8.17 (9.46)	16.98 (23.74)
ECHAM5 A1b	85.22 (9.94)	−47.79 (2.54)	1.38 (3.95)	−0.06 (0.66)	−17.52 (23.02)	19.86 (28.06)
ECHAM5 A2	74.07 (8.72)	−51.81 (2.00)	1.37 (3.95)	−0.05 (0.63)	−14.4 (18.14)	7.81 (26.82)
ECHAM5 B1	70.83 (6.87)	−56.77 (2.28)	1.28 (4.11)	−0.04 (0.55)	−11.52 (20.67)	2.50 (28.29)
Statewide						
CCCMA A1b	228.87 (19.72)	−140.53 (34.87)	7.50 (6.51)	−0.07 (0.06)	−22.01 (19.51)	66.25 (33.64)
CCCMA A2	230.22 (21.70)	−152.99 (22.65)	7.59 (9.03)	−0.16 (0.15)	−49.41 (44.76)	27.66 (34.03)
CCCMA B1	225.52 (12.26)	−162.6 (28.69)	6.71 (5.73)	−0.11 (0.08)	−32.05 (25.1)	30.77 (29.51)
ECHAM5 A1b	268.84 (24.88)	−169.11 (36.13)	7.68 (8.95)	−0.17 (0.16)	−52.78 (47.97)	46.77 (49.46)
ECHAM5 A2	248.08 (25.25)	−173.39 (26.52)	7.70 (7.41)	−0.16 (0.18)	−47.95 (54.4)	26.58 (57.60)
ECHAM5 B1	240.14 (18.39)	−184.27 (27.76)	6.79 (5.75)	−0.12 (0.16)	−36.28 (47.1)	19.47 (50.97)

Notes: Numbers in parenthesis indicate inter-annual standard deviation. Positive numbers indicate uptake of C into upland ecosystems and negative numbers indicates losses of C.

LCC consistent with statewide results (ECHAM5 B1). The highest gains in soil C were for the CCCMA A1b scenario among all of the LCCs (consistent with those observed statewide). Similar to the pattern for total C storage, the climate scenario that resulted in the smallest gains in soil C storage varied among the LCCs, with only the Western Alaska LCC consistent with statewide results (ECHAM5 B1). The highest gains in vegetation C storage were for the ECHAM5 A2 scenario (consistent with those observed statewide) for all the LCCs except the North Pacific LCC, which had the highest gains for ECHAM5 A1b. For all the LCCs, the lowest gains in vegetation C were for CCCMA B1 (consistent with those observed statewide).

For all the LCCs, NPP increased under all scenarios (Table 4), as did fire emissions, except for Western Alaska LCC in one scenario (CCCMA A1b). The change in HR varied substantially among the LCCs. HR was estimated to increase for the North Pacific LCC in all scenarios and to increase in the Arctic LCC except for two scenarios (CCCMA A2 and ECHAM5 A2). In contrast, HR decreased in all scenarios for the Northwest Boreal LCC and in all but two scenarios for the Western Alaska LCC (ECHAM5 A2 and B1). Mean NECB was positive, and increased for all LCCs and all scenarios (Table 4).

Partitioning the response of upland C balance to climate change among drivers

The response of upland C stocks and permafrost to changes in environmental drivers.—Statewide, the projected increase in atmospheric CO_2 and climate change promoted an

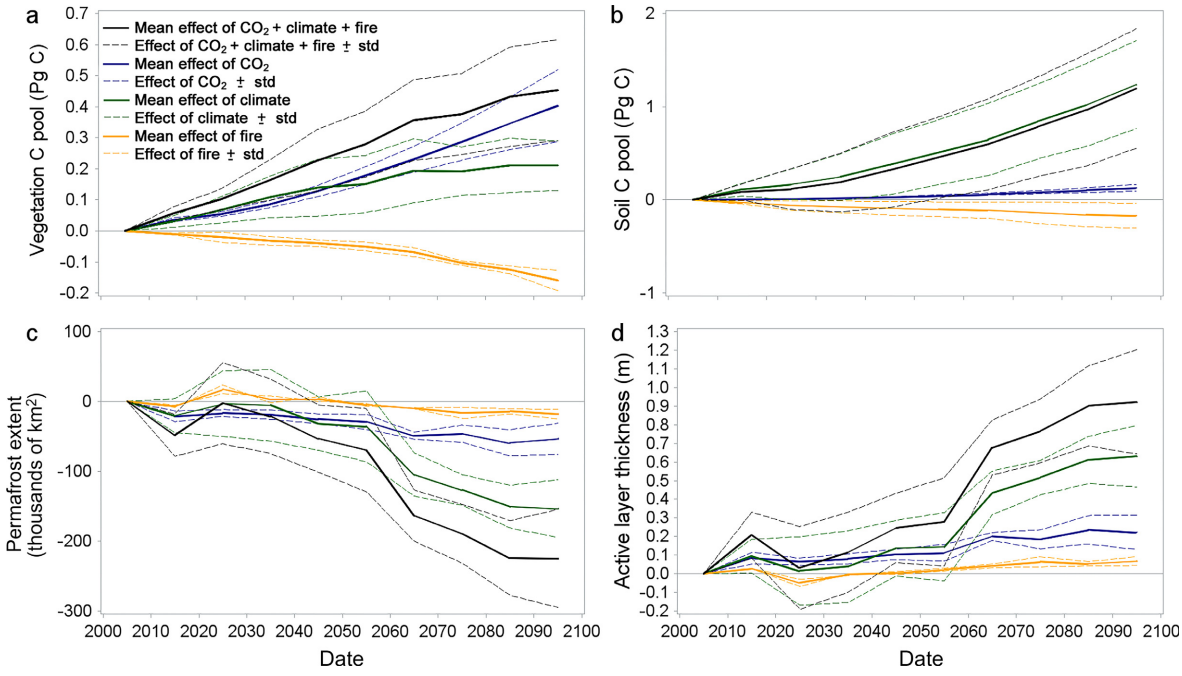

FIG. 4. Anomaly from the baseline simulation (constant atmospheric CO_2, climate, and fire regime) quantifying the cumulative effects of increasing atmospheric CO_2 (blue line), change in climate (green line), and change in fire regime (orange line) on (a) total vegetation carbon stocks, (b) total soil carbon stocks, (c) total extent of the near surface permafrost (within 3 m from the surface), and (d) active layer thickness across Alaska from 2010 through 2099. The black line represents the cumulative effect of increases in atmospheric CO_2, changes in climate, and changes in the fire regime. The thick solid lines represent the mean among scenarios and the dotted lines represent the mean ± SD.

increase in both vegetation and soil C stocks (Fig. 4a, b). Compared to the baseline simulation, vegetation C stocks tended to be more responsive to increasing atmospheric CO_2 (Fig. 4a, blue line) than climate change (Fig. 4a, green line), while soil C stocks were more responsive to climate warming than increasing atmospheric CO_2 (Fig. 4b). Increases in area burned decreased both vegetation and soil C stocks (Fig. 4a, b, yellow lines). Climate warming was primarily responsible for losses of permafrost (Fig. 4c) and deepening of the active layer (Fig. 4d).

The effect of CO_2 fertilization on NPP and HR.—The effects of increasing atmospheric CO_2 on ecosystem C fluxes were evaluated by comparing decadal averages from 2010 to 2099 of the baseline simulation (constant atmospheric CO_2, climate and fire regime) with those from simulations using increasing atmospheric CO_2, detrended climate and constant fire regime (CO_2 simulations). Increasing atmospheric CO_2 caused a significant increase in NPP compared to baseline ($F_{1,136} = 2291.55$, $P < 0.0001$) that was different among the LCC regions ($F_{4,136} = 34.82$, $P < 0.0001$). The sensitivity of NPP varied between 3.8% and 7.7% per 100 part per million by volume (ppmv) increase in atmospheric CO_2 among the LCCs (Fig. 5a). The uncertainty of these sensitivities (i.e., the standard error of the slope between change in NPP and change in atmospheric CO_2) varied between 0.06% to 0.14% per 100 ppmv among the LCCs (standard errors are 0.10%, 0.14%, 0. 06%, and 0.10% per 100 ppmv for the Arctic, the North Pacific, the Northwest Boreal, and the Western Alaska LCCs, respectively). The relative increase in NPP was greatest in the tundra-dominated regions of the Arctic and Western Alaska LCCs, intermediate for the Northwest Boreal LCC and the lowest for the North Pacific LCC. For all regions however, the relative increase in NPP diminished with increasing atmospheric CO_2, following a quadratic relationship (Fig. 5a). Increasing atmospheric CO_2 also induced a linear increase in heterotrophic respiration compared to the baseline ($F_{1,136} = 11.21$, $P = 0.0008$). Differences among LCC regions in the slope of the relationship were not significant ($F_{4,136} = 0.53$, $P = 0.6646$). A 100 ppmv increase in atmospheric CO_2 induced a 2.7% ± 0.86% per 100 ppmv (mean ± SE) increase in HR (Fig. 5b).

The effects of climate change on decadal averages of NPP and HR.—The effects of changing climate on ecosystem C fluxes were evaluated by comparing decadal averages from 2010 to 2099 of the simulations with increasing atmospheric CO_2 and constant climate and fire regime (CO_2 simulations) with those from simulations with increasing atmospheric CO_2, changing climate and constant fire regime (CO_2 + climate simulations). Increases in air temperature resulted in a significant increase in NPP (Table 5); this increase was not significantly different among LCC regions, although there was a significant

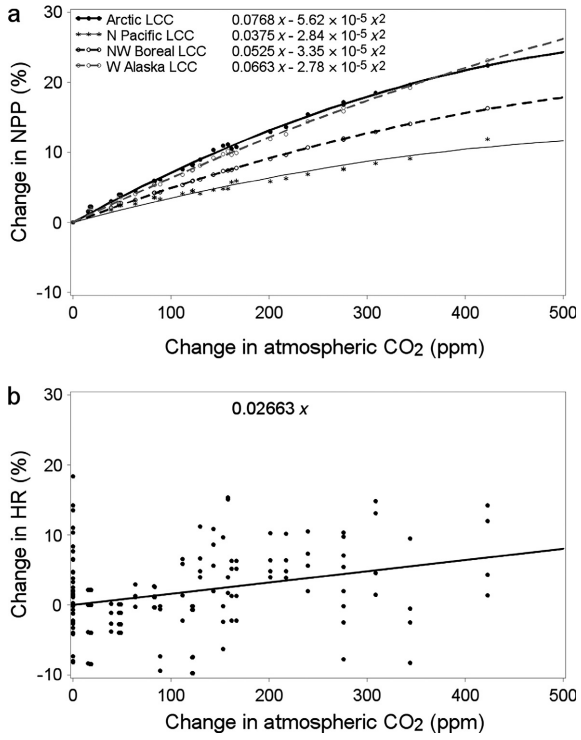

FIG. 5. Relationship between (a) relative change in NPP and (b) relative change in heterotrophic respiration (HR) with atmospheric CO_2 from the baseline (simulations with constant atmospheric CO_2). Different symbols and lines are depicted for each different LCC region. Each point represents the difference of decadal averages between the baseline and each atmospheric CO_2 scenarios. Quadratic relationships are shown for relative change in NPP for each LCC.

interaction between changes in air temperature and LCC regions. The sensitivity of NPP ranged between 2.17% and 4.42% per °C increase in air temperature among the LCCs. The uncertainty of these sensitivities (i.e., the standard error of the slope between change in NPP and change in temperature) varied between 0.33% to 0.42% per °C among the LCCs. The response of NPP to climate warming tended to be greater in the Arctic and North Pacific LCCs than in the Western Alaska and Northwest Boreal LCCs (Fig. 6a). Increases in air temperature caused significant increases in HR (Table 5). While the magnitude of the change in HR, independent of the change in temperature, was significantly different among LCCs (ranging from −10.06% to −1.13%), the response to warming (i.e., the slope between change in HR and change in air temperature) was not (Table 5). The overall response of HR to changes in air temperature follows an upward sloping quadratic relationship (Fig. 6b). The standard error associated with this relationship was 0.091% per °C. Projected changes in precipitation, net incoming radiation, and vapor pressure had no significant effect on NPP or HR (results not shown), except for a positive effect of increasing annual precipitation on change in NPP for the North Pacific LCC where the projected increase in precipitation during the 21st century was the largest (sensitivity is 0.023% per mm with standard error of 0.002% per mm; $P < 0.001$; Fig. 6c).

The increase in HR in response to climate warming was associated with two co-occurring processes: (1) the increase of organic C input from litter fall to the organic layer (Fig. 7a) and (2) the increase in soil temperature (Fig. 7b) and associated deepening of the active layer (Fig. 7c). The relationship between HR and litterfall was linear ($F_{1,215} = 3112.34$, $P < 0.001$), while the relationship between HR and soil temperature followed a cubic relationship ($F_{1,215} = 464.72$, $P < 0.001$). The relationship between HR and the active layer thickness was also linear ($F_{1,215} = 652.76$, $P < 0.001$), but the variability of this relationship increases with active layer thickness. Below about 4.8 m, the active layer thickness has no significant influence on HR (mostly in the North Pacific LCC, where permafrost is very isolated).

No significant effect of warming on the Net Ecosystem Productivity (NPP − HR) was detected.

The effects of climate change on the seasonal dynamics of snow cover and NPP.—The effects of projected climate change on the seasonal dynamics of snow cover and NPP were evaluated by comparing the baseline scenario with the scenarios for increases in atmospheric CO_2 and changing climate (CO_2 + climate scenarios) during the final decade of the projection period (2090–2099). Compared to the baseline, the increase in atmospheric CO_2 and climate change caused an increase in the seasonal maximum of NPP in all LCC regions. Changes in the magnitude of seasonal maximum NPP compare to the baseline were substantial in the Arctic LCC (Fig. 8a; 17.92 ± 8.54 g C·m^{-2}·yr^{-1} [mean ± SD]) and the North Pacific LCC (Fig. 8d, 5.02 ± 5.71 g C·m^{-2}·yr^{-1}). In the Northwest Boreal LCC, the seasonal maximum NPP

TABLE 5. Effects of LCC region, changes in air temperature (Δtair), changes in precipitation (Δprec) and the interaction between LCC region and changes in air temperature or precipitation on relative changes in net primary productivity (ΔNPP) and heterotrophic respiration (ΔHR).

	ΔNPP (%)					ΔHR (%)				
Source	*n*	MS	df	*F*	*P*	*n*	MS	df	*F*	*P*
LCC	3	75.8	4,208	1.56	0.201	**3**	**911.5**	4,208	**4.6**	**0.004**
Δtair (°C)	**1**	**3540.9**	1,208	**72.76**	**<0.001**	**1**	**3750.5**	1,208	**18.93**	**<0.001**
LCC × Δtair (°C)	**3**	**319.9**	3,208	**6.57**	**<0.001**	**3**	408.9	3,208	1.76	0.157

Note: Statistics in bold indicate significant effect.

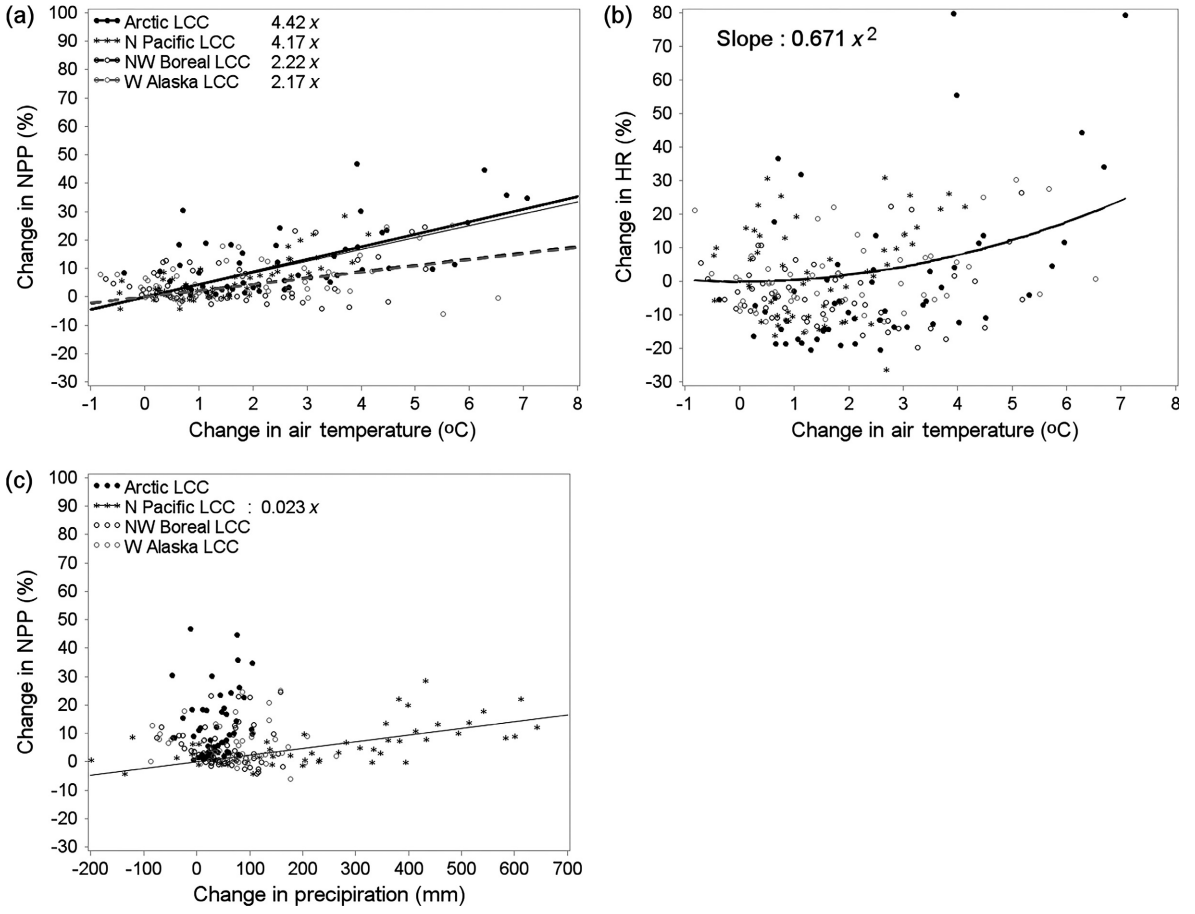

FIG. 6. Relative change in (a) NPP and (b) HR in response to changes in air temperature, and (c) change in NPP in response to changes in annual precipitation. Different symbols and line correspond to different LCC regions in panels a and c, as there is a significant interaction between relative changes in NPP and changes in air temperature or annual precipitation. Each point represents a decadal average. Significant relationships are indicated next to symbols and LCC names, with x standing for the change in precipitation.

occurred in May instead of June (Fig. 8b). Climate change also resulted in an earlier start of the growing season in all the LCCs that coincided with earlier snowmelt (Fig. 8). Similarly, climate change resulted in a later end of growing season that coincided with later snow return in the fall (Fig. 8).

The effects of fire on NPP, HR, and NECB.—The effects of a changing fire regime on ecosystem C fluxes were evaluated by comparing changes in decadal NPP, HR, and NECB between simulations with increasing atmospheric CO_2, changing climate and constant fire regime (CO_2 + climate scenarios), and with simulations with increasing atmospheric CO_2, changing climate and changing fire regime (CO_2 + climate + fire scenarios). Relative changes in fire emissions were not computed as baseline fire emission could equal zero in LCC regions with low fire activity.

Increases in area burned caused significant decreases in NPP ($F_{1,215} = 48.48$, $P < 0.001$; Fig. 9a) and HR ($F_{1,215} = 285.87$, $P < 0.001$; Fig. 9b), and significant increases in fire emissions ($F_{1,215} = 394.87$, $P < 0.001$; Fig. 9c). The effect of increasing area burned on these C fluxes was significantly different among LCC regions. The largest responses to increasing area burned were observed in the Northwest Boreal and Western Alaska LCCs. Statewide, a 1% increase in area burned resulted in a 0.39% and 2.87% decrease in NPP and HR, respectively, and an increase of 9.55 g $C \cdot m^{-2} \cdot yr^{-1}$ in fire emissions. The net effect of fire in the projection period on NECB was to decrease C storage ($F_{1,215} = 62.18$, $P < 0.001$; Fig. 9d), and at the statewide level, fire decreased NECB by 0.010 Tg C/yr to 0.018 Tg C/yr among the climate scenarios we evaluated (see also Fig. 4a, b).

DISCUSSION

Upland ecosystems occupy 84% of the terrestrial land surface in Alaska (i.e., 1,237,774 km^2), and thus have played an important role in the past and are expected to continue to play an important role in the future in the overall C balance of the state. In this study, we used a modeling framework to estimate the historical and future

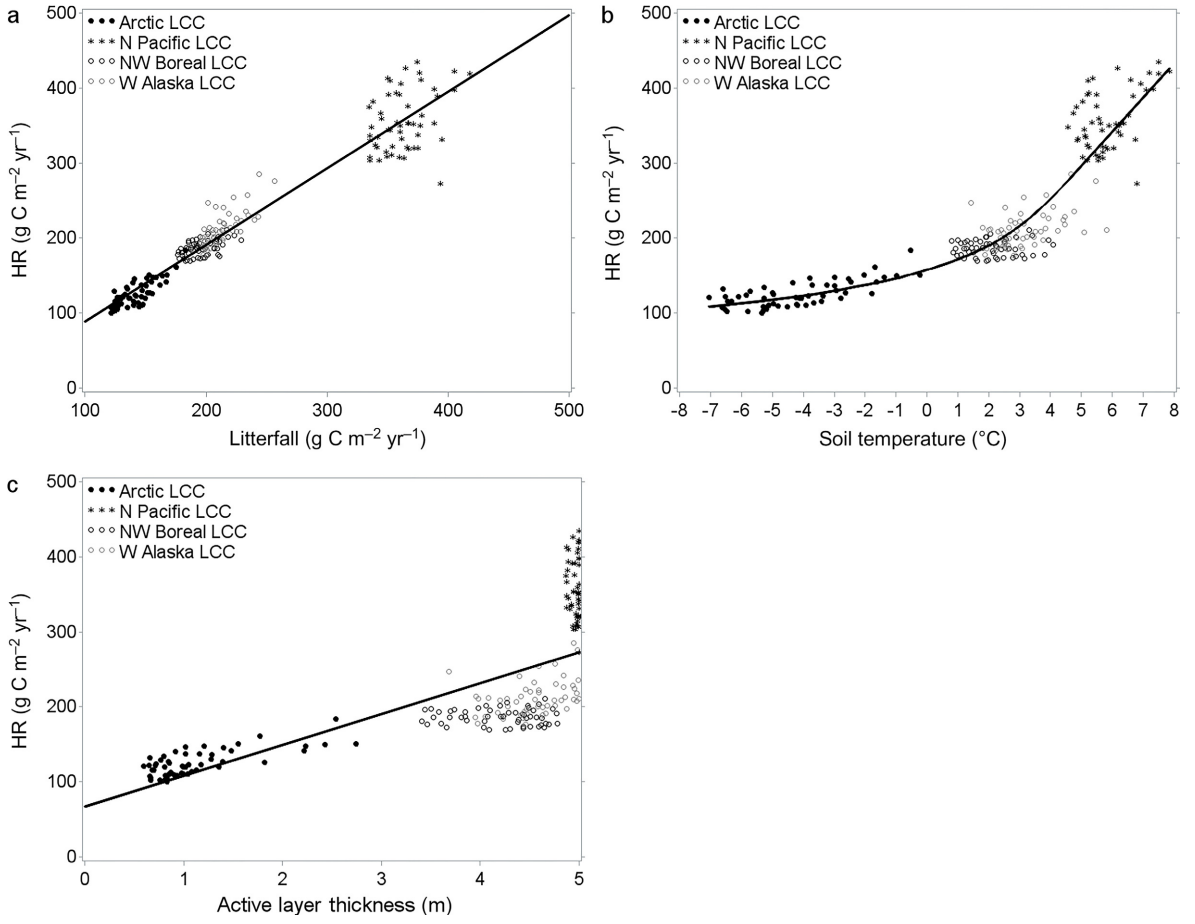

FIG. 7. Relationship between HR and (a) litterfall, (b) annual mean 5-m soil temperature, and (c) active layer thickness between 2010 and 2099 for each LCC region. The black line represents the relationship between HR and the three environmental variables, without taking into account the differences between LCCs. Each point represents a decadal average. Significant relationships are indicated next to symbols and LCC names, with x standing for the change in precipitation.

C dynamics of upland ecosystems in Alaska. Below we discuss our key findings about the magnitude and changes in C storage separately for the historical and future periods of our analyses. We then discuss the relative role of factors driving these dynamics in upland ecosystems of Alaska and the limitations and uncertainties of this assessment.

Historical C dynamics in Alaska uplands

We estimate that upland ecosystems of Alaska currently store more than 50 Pg C, over 90% of which is in soils. The modeled density of soil organic C storage (~38,000 g C/m^2) is higher than recent estimates of soil C density for the 0–1 m soil column (i.e., mean 26,517 g C/m^2, 95% CI 25,002–28,032 g C/m^2) for the circumpolar region (Hugelius et al. 2013, 2014, Michaelson et al. 2013). This difference can be largely explained by the fact that the soil column considered for this assessment included C stored in the organic layer plus 1 m of mineral soil, resulting in a soil column thicker than the 0–1 m soil column commonly used for circumpolar assessments. The mean organic layer thickness by the end of the historical period was estimated to be 29.7 ± 25.3 cm (mean ± SD; among LCC regions), bringing the total thickness of the soil column to 1.3 m. To compensate for this difference, we added 29.7% of the 1–2 m deep soil C estimates to the 0–1 m estimates from Hugelius et al. 2014 (considering that soil C density is homogeneous between 1 and 2 m), bringing the global soil C density to 32,669 g C/m^2, which lowers the over-estimation of soil C density in this assessment to 16%. In the Northwest Boreal LCC region, our estimates for vegetation C (3,484 g C/m^2) and soil C (27,324 g C/m^2) stocks are close to estimates of C stocks in the Alaska boreal forest by Bradshaw and Warkentin (2015; 5,770 and 22,120 g C/m^2, respectively).

Our analysis indicates that, statewide, Alaska gained C at a rate of 3.26 Tg C/yr between 1950 and 2009, but some regions of the state gained C while others lost C. Gains occurred in tundra and coastal forest regions of Alaska primarily driven by increases in NPP. Other studies have reported increases in NPP in arctic regions in response to warming (Epstein et al. 2008, Myers-Smith

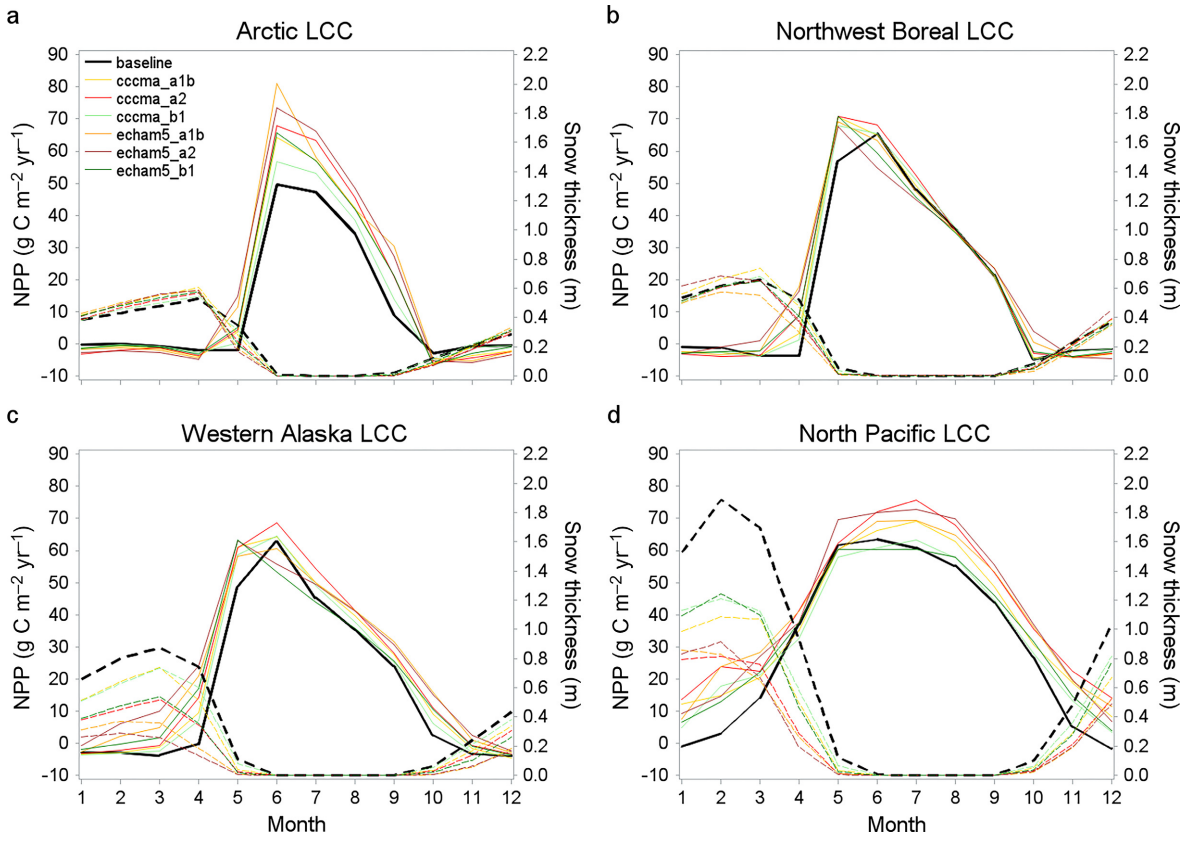

FIG. 8. Seasonal dynamic of monthly NPP (solid line) and snow cover thickness (dotted lines) for each LCC region. The thick black lines represent baseline simulation. Each colored line represents decadal average of monthly data for each climate scenario for the period 2090–2099. The difference between the baseline and the other scenarios represents the combined effect of climate change and increasing atmospheric CO_2. Significant relationships are indicated next to symbols and LCC names, with x standing for the change in precipitation.

et al. 2011, Bonfils et al. 2012). In the Arctic LCC, our estimates are within the range of NPP and HR reported by a recent model inter-comparison. That study used 40 terrestrial ecosystem models to assess terrestrial C cycle uncertainty in Arctic Alaska (Fisher et al. 2014). In 2002 and 2003, we estimate NPP and HR to be 118 g $C{\cdot}m^{-2}{\cdot}yr^{-1}$ and 97 g $C{\cdot}m^{-2}{\cdot}yr^{-1}$, respectively, and Fisher et al. (2014) estimated NPP and HR to be 140 ± 300 g $C{\cdot}m^{-2}{\cdot}yr^{-1}$ (mean ± SD) and 140 ± 200 g $C{\cdot}m^{-2}{\cdot}yr^{-1}$, respectively, for the same period. In the North Pacific LCC, gains from increased forest growth dominate the C balance as the C loss from logging activities would have to more than double to drive NECB negative.

The losses of C during the historical period occurred in upland ecosystems of the boreal forest region of Alaska, and were primarily driven by changes in fire regime. The losses of C in uplands of the boreal forest region of Alaska are consistent with remote sensing (Goetz et al. 2007, Beck and Goetz 2011) and other analyses (Barber et al. 2000, Turetsky et al. 2011, Walker and Johnstone 2014) that conclude that C gains in this region are limited by drought stress and fire mortality. Our analyses indicate that about 10 yr of statewide C accumulation in uplands can be lost in a single large fire year through fire emissions. The estimated losses of C in this region are occurring because fires are becoming more frequent. Kasischke et al. (2002) estimate that since 1980, Alaska experienced three to four large fire years per decade, compared to one to two large fire years per decade between 1960 and 1980. During the last decade of the historical period, we estimate that about 86% of the statewide C fire emissions occurred in uplands of the Northwest Boreal LCC (~50 g $C{\cdot}m^{-2}{\cdot}yr^{-1}$). For black spruce forest ecosystems, the most vulnerable ecosystems to fire in this LCC, we estimate that fire emissions were 71.4 g $C{\cdot}m^{-2}{\cdot}yr^{-1}$, which is similar to the estimate by Turetsky et al. (2011; 76.2 ± 10.24 g $C{\cdot}m^{-2}{\cdot}yr^{-1}$; mean ± SE).

Future C dynamics in Alaska uplands

Our analysis suggests that, by the end of the 21st century, C storage in upland ecosystems of Alaska will increase by 3.4–11.7% among the climate scenarios we evaluated. Vegetation C is estimated to increase between 11.7% and 23.8%, and soil C between 2.2% and 11.2%. At the statewide level, these increases largely occurred

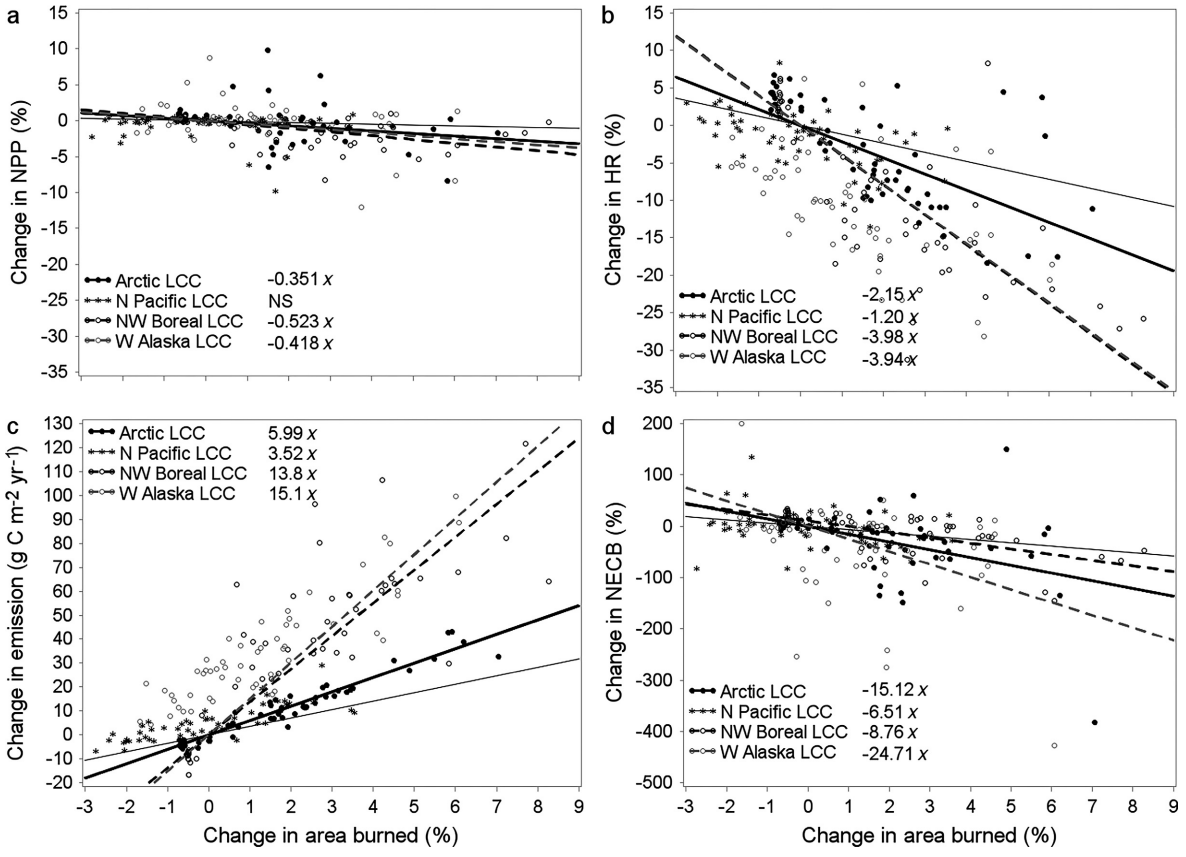

FIG. 9. (a) Relative change in NPP (b) in HR, (c) in pyrogenic emissions and (d) in NECB in response to change in relative area burned. Different symbols and line correspond to different LCC region. Each point represents a decadal average per LCC region, per scenario. Significant relationships are indicated next to symbols and LCC names, with x standing for the change in precipitation.

because of the mean increase in NPP and the mean decrease in HR during the projection period in comparison to the historical period. The increase in NPP was primarily driven by the response of NPP to increases in atmospheric CO_2 even though the response is relatively modest (4.8% per 100 ppmv at the statewide level). The effect is substantially lower than the estimates from four FACE experiments in temperate forest stands (Norby et al. 2005; 13% per 100 ppm) and in comparison to most other models applied over the northern permafrost region (McGuire et al. 2016) because of nitrogen limitation on the CO_2 fertilization response in DOS-TEM (Euskirchen et al. 2009). It is also important to note that the response of NPP to increases in atmospheric CO_2 in our simulations becomes less sensitive as atmospheric CO_2 increases (Fig. 5). The main reasons of the decrease in sensitivity of NPP to atmospheric CO_2 are the Michaelis-Menten function between GPP and atmospheric CO_2 and the constraint of nitrogen availability on GPP formulated in DOS-TEM (Raich et al. 1991, McGuire et al. 1992, Euskirchen et al. 2010).

The increase in NPP was also driven by increases in air temperature, and the level of sensitivity in our simulations is consistent with that reported by warming experiments conducted in Arctic Alaska (Chapin et al. 1995, Piao et al. 2013). The increased NPP was also caused by a longer length of the growing season resulting from earlier snowmelt and later snowfall. These seasonal changes in response to climate warming are in line with previous studies (Groisman et al. 1994, Euskirchen et al. 2006, 2016). While NPP is more sensitive to air temperature than HR over the 21st century in our simulations, our simulations suggest that HR will ultimately become more sensitive to air temperature because of its upward curvilinear relationship with temperature that is being driven by both increasing soil temperature and deepening active layer, the latter of which exposes frozen organic matter to decomposition (see also Hayes et al. 2014, Koven et al. 2015, Schuur et al. 2015). Thus, at the statewide level and over a longer time period than our simulations, our analyses would suggest that the decreasing CO_2 sensitivity of NPP and the increasing sensitivity of HR to air temperature will ultimately lead to a source of CO_2 to the atmosphere from upland ecosystems of Alaska. This is consistent with other analyses that have been conducted in the northern permafrost region by models that represent soil C vertically, which suggest that soil C loss will be much greater between 2100 and 2200 than between 2000 and 2100 (Schuur et al. 2015).

Fire is an important disturbance that has a complicated effect on the projected increases in C storage in our simulations. Mean annual area burned in the projection period ranged from −81.5% to +169.3% of that during the historical period. Our analysis shows that increased area burned tends to decrease NPP, decrease HR, and increase fire emissions. The decrease in NPP is associated with tree mortality and the decrease in HR following wildfire is related to the partial or total burning of the organic horizons during combustion and the decrease in C input from vegetation litterfall. In fire-prone regions, our study suggests that decreases in HR from wildfire can be greater than increases resulting from warming (and increasing vegetation productivity) associated with increasing CO_2 and climate change in those regions. As a result, HR decreases during the projection period in the two largest and most fire-prone LCC regions, namely the Northwest Boreal and the Western AK LCCs, where on average 56.2% ± 13.5% and 23.2% ± 11.4% (mean ± SD among climate scenarios) of the area burns every 100 yr, respectively (Rupp et al. 2016). Statewide, the decrease in HR from these two LCCs is greater than the increase in HR projected in the less fire-prone Arctic and the North Pacific LCCs, resulting in an overall decrease of 9.1% in HR (8.6% SD among climate scenarios) in comparison to the historical period. The net result is that increases in fire decrease NECB and cause losses in both vegetation and soil C. Whether fire will continue to limit gains (or promote losses) of C from upland ecosystems of Alaska depends on feedbacks between vegetation composition and the occurrence of fire. The increase in fire severity and fire frequency can promote the establishment of deciduous forest (e.g., Johnstone et al. 2010b, Pastick et al. 2017). Because deciduous forest is less flammable than black spruce forest (Bernier et al. 2016), the transition from evergreen to deciduous vegetation could result in less fire on the landscape in the latter part of this century. This interaction between vegetation composition and fire regime is represented in this study since ALFRESCO represents the effect of fire severity on post-fire vegetation succession and the feedback of vegetation composition on fire regime (see Pastick et al. this feature). However, since the vegetation composition in DOS-TEM is considered static, the direct effect of changes in vegetation composition on carbon dynamics was not included.

Across the projection period, NECB was larger in tundra-dominated regions (the Arctic and Western Alaska LCCs) and the North Pacific LCC than in the Northwest Boreal LCC. The increase in fire was the primary reason for the more muted response of the Northwest Boreal LCC in comparison to the other LCCs, where the responses of NPP to increases in atmospheric CO_2 and increased temperature primarily drove the larger NECB. Regions of largest uncertainties among the climate scenarios, for example the Yukon-Kuskokwim Delta or the northern Seward Peninsula, were also regions that experienced the largest increase in length of the growing season, as shown in Fig. S2 of Pastick et al. (this feature).

In past syntheses of regional C dynamics, the role of aerated soils as a sink for CH_4 has generally been neglected. Consistent with field observations (Whalen and Reeburgh 1990, Moosavi and Crill 1997, Martineau et al. 2010), this assessment shows that biogenic CH_4 fluxes in upland Alaska were a net sink from the atmosphere. Other analyses suggest that biogenic CH_4 sequestration in upland soils should increase during the 21st century (Zhuang et al. 2013) in response to an increase in litter organic C input and soil temperature (Walter and Heimann 2000, Hofmann et al. 2016) and an increase in unsaturated soil volume resulting from permafrost thaw and deepening the water table (Whalen and Reeburgh 1990, Zhuang et al. 2004). However, our analysis suggests that the effects of climate change on biogenic CH_4 sequestration would be trivial at the regional scale, and that CH_4 balance in uplands would primarily be driven by pyrogenic emissions of CH_4. The pyrogenic CH_4 loss from uplands ecosystems is relatively minor, as it represents less than 0.1% of upland NPP.

Limitation and uncertainties of projections of C balance in upland Alaska

This assessment of C dynamics in upland ecosystems of Alaska provided estimates of the uncertainty associated with forcing data, i.e., atmospheric CO_2 for three emission scenarios and climate projections from two global circulation models, on the regional C balance. Statewide, although the variability of NECB among the six climate scenarios was substantial (SD = 17.2 Tg C/yr), all scenarios predicted uplands to be a C sink by the end of the 21st century. The uncertainty of NECB associated with CO_2 emission scenarios (SD = 17.6 Tg C/yr) was larger than the uncertainty associated with GCMs (SD = 7.5 Tg C/yr). As mentioned previously, the effect of forest logging in the North Pacific LCC was not included in the future projections as explicit projections were not available at the time this assessment was conducted. Yet, from the historical estimates, the total export of C from logging activities were quite small (i.e., 1.6 Tg C/yr). If projected to be constant over the 21st century, these exports would have had a minor effect on the estimated statewide C sink (i.e., 5.2% decrease of NECB on average, SD = 2.1% among climate scenarios). Furthermore, a recent attribution analysis quantifying the relative effect of logging and climate change on forest C stocks in the North Pacific LCC suggested that the effect of harvesting on forest C stocks for the 21st century was more than 27 times smaller than the effect of climate change only (for the CCCMA-A1b scenario; Zhou et al. 2016).

In addition to forcing data, model structure and process representations can be a significant source of uncertainty in ecosystem carbon projections. A recent model comparison of the historical carbon balance in Alaska, compared model inter-comparison projects using similar or different forcing data and estimated that uncertainty resulting from differences in model structure and process

representations can be larger than uncertainty resulting from differences in forcing data (Fisher et al. 2014). DOS-TEM explicitly represents processes that have been identified as critical to represent in high latitude ecosystems (McGuire et al. 2012, 2016, Koven et al. 2015, Luo et al. 2016). These processes include (1) soil thermal regime and permafrost dynamics and their effects on soil C dynamics (Yi et al. 2009b), (2) nitrogen limitation on vegetation productivity (Euskirchen et al. 2010), and (3) and organic layer dynamics on soil environmental and biogeochemical processes (Yi et al. 2009a, 2010). However, additional processes not represented in the modeling framework used in this study can affect ecosystem dynamics at the regional level, and may change in response to climate change.

The biogeochemical models used in this assessment did not include a dynamic vegetation model, i.e., vegetation distribution was static after initialization. Yet, with climate change and change in disturbance regime, changes in vegetation composition are ongoing (e.g., Sturm et al. 2001, Tape et al. 2006) and expected to continue over the coming decades in the boreal and the Arctic regions (e.g., Pastick et al. 2017), with the potential to cause significant changes in the regional carbon balance. In the arctic region, climate-related shrubification in the Arctic (Myers-Smith et al. 2011) is projected to offset the loss of shrub tundra from increasing fire frequency (Pastick et al. 2017), and result in a decrease in soil temperature that can slow down decomposition of soil organic matter and reduce heterotrophic respiration (Sistla et al. 2013). The transition from graminoid to shrub tundra can also cause an increase in vegetation productivity and vegetation biomass (Shaver and Chapin 1991). In boreal forest, the projected increase in wildfire frequency and severity can result in large-scale transition from spruce-dominated forest to deciduous-dominated forest (e.g., Johnstone et al. 2010b), which can lead to an increase in vegetation productivity and litter quality and an increase in soil temperature and decomposition rates (Melvin et al. 2015).

The current assessment is considering soil biogeochemical processes occurring in the organic layer and the first meter of the mineral soil. Yet, substantial amount of organic C can be stored below this depth (Harden et al. 2012a) and, with active layer deepening, can become unfrozen and be exposed to decomposition (Schuur et al. 2009). Additionally, lateral loss of dissolved organic C (DOC) from terrestrial to aquatic ecosystems are not taken into account in the modeling framework (Stackepoole et al. 2017). Yet, previous model simulations estimated that DOC loss can have a substantial effect on the regional C balance, reducing the strength of the C sink in the Arctic region (McGuire et al. 2010, Kicklighter et al. 2013). Finally, the degradation of permafrost in uplands may trigger thermal-erosion processes and the formation of features such as active layer detachments or retrogressive thaw slumps (Balser et al. 2014) with dramatic changes on local hydrology and vegetation that could affect substantially ecosystem C balance (Jensen et al. 2014).

Finally, studies quantifying the actual proportion between the quantity of wood harvested (and exported out of the ecosystem) and the residues left on site in Northern Pacific forests are very scarce. Given that clear cutting is the most common harvest practice in the region (Cole et al. 2010), we used the highest proportion of cutting intensity estimated by Deal and Tappeiner (2002) to estimate C exported out of the ecosystem from timber harvest. Yet, our study might have underestimated the proportion of wood left on site after cutting. An older study by Howard and Setzer (1989) estimates that only 43.3–51.3% of the forest volume is exported out of the ecosystem. A mean harvest rate of 47.3% would decrease the total C exported as timber from 1.6 Tg C/yr to 0.80 Tg C/yr and would increase the historical C sink from 3.26 Tg C/yr to 4.06 Tg C/yr.

Conclusion

This assessment of C dynamics in upland ecosystems of Alaska is unique in that it explicitly separates uplands from wetlands C dynamics. As in any assessment, there are limitations and uncertainties. Key limitations include (1) the treatment of land cover as static in the projection period, and (2) the lack of consideration of disturbances in addition to fire such as those caused by insects and thawing of ice-rich permafrost and associated soil subsidence. It is well known that increased fire disturbance has the potential to increase the cover of deciduous forest at the expense of spruce forest (Johnstone et al. 2010a,b). It is also expected that shrub tundra will expand at the expense of graminoid tundra (Myers-Smith et al. 2011). Insects and disease also substantially affect forest productivity in the Alaska boreal forest (Verbyla 2011), and there is evidence that insect disturbance is increasing in Alaska (Parent and Verbyla 2010). Finally, degradation of ice-rich permafrost in uplands has the potential to alter C cycling in the northern permafrost region (Grosse et al. 2011, Olefeldt et al. 2016). Model modifications to deal with these issues are currently being developed so that these issues can be better addressed in future assessments. Despite these limitations, our study provides important insights on regional vulnerability of C storage in Alaska. In particular, our study indicates that projected C sequestration in the Northwest Boreal LCC would be weakest among the LCCs. This suggests that this region would be most vulnerable to becoming a C source during the remainder of the 21st century in response to other disturbances and harvesting that we did not consider. Finally, even if upland ecosystems as a whole are able to sequester C throughout the 21st century, our analysis indicates that any increased C sequestration in upland ecosystems of Alaska during the 21st century is likely to be transitional as NPP becomes less sensitive to increases in atmospheric CO_2 and HR increases due to increase in C input from the vegetation, warmer soil, and a deeper active layer.

Acknowledgments

This research was funded by the U.S. Geological Survey (USGS) Land Change Science Program. Additional support was provided by (1) the Alaska Climate Science Center through Grant/Cooperative Agreement G10AC00588 from the U.S. Geological Survey and (2) the National Science Foundation and the USDA Forest Service through the Bonanza Creek Long Term Ecological Research Program. Any use of trade, firm, or product names is for descriptive purposes only and does not imply endorsement by the U.S. Government.

Literature Cited

Abbott, B. W., et al. 2016. Biomass offsets little or none of permafrost carbon release from soils, streams, and wildfire: an expert assessment. Environmental Research Letters 11:034014.

Ainsworth, E. A., and S. P. Long. 2005. What have we learned from 15 years of free-air CO2 enrichment (FACE)? A meta-analytic review of the responses of photosynthesis, canopy properties and plant production to rising CO_2. New Phytologist 165:351–372.

Alaback, P. B. 1982. Dynamics of understory biomass in Sitka spruce-western hemlock forests of southeast Alaska. Ecology 63:1932–1948.

Balser, A. W., J. B. Jones, and R. Gens. 2014. Timing of retrogressive thaw slump initiation in the Noatak Basin, northwest Alaska, USA. Journal of Geophysical Research—Earth Surface 119:1106–1120.

Balshi, M. S., et al. 2007. The role of historical fire disturbance in the carbon dynamics of the pan-boreal region: A process-based analysis. Journal of Geophysical Research—Biogeosciences 112:2156–2202.

Balshi, M. S., A. D. McGuirez, P. Duffy, M. Flannigan, J. Walsh, and J. Melillo. 2009. Assessing the response of area burned to changing climate in western boreal North America using a multivariate adaptive regression splines (MARS) approach. Global Change Biology 15:578–600.

Barber, V. A., G. P. Juday, and B. P. Finney. 2000. Reduced growth of Alaskan white spruce in the twentieth century from temperature-induced drought stress. Nature 405:668–673.

Beck, P. S. A., and S. J. Goetz. 2011. Satellite observations of high northern latitude vegetation productivity changes between 1982 and 2008: ecological variability and regional differences. Environmental Research Letters 6:045501.

Bekryaev, R. V., I. V. Polyakov, and V. A. Alexeev. 2010. Role of polar amplification in long-term surface air temperature variations and modern arctic warming. Journal of Climate 23:3888–3906.

Bernier, P. Y., S. Gauthier, P.-O. Jean, F. Manka, Y. Boulanger, A. Beaudoin, and L. Guindon. 2016. Mapping local effects of forest properties on fire risk across Canada. Forests 7:157. https://doi.org/10.3390/f7080157

Bhatti, J. S., M. J. Apps, and H. Jiang. 2010. Influence of nutrients, disturbances and site conditions on carbon stocks along a boreal forest transect in central Canada. Plant and Soil 242:1–14.

Bieniek, P. A., et al. 2015. Climate drivers linked to changing seasonality of Alaska coastal tundra vegetation productivity. Earth Interactions 19:19.

Binkley, D. 1982. Nitrogen-fixation and net primary production in a young Sitka alder stand. Canadian Journal of Botany 60:281–284.

Bonfils, C. J. W., T. J. Phillips, D. M. Lawrence, P. Cameron-Smith, W. J. Riley, and Z. M. Subin. 2012. On the influence of shrub height and expansion on northern high latitude climate. Environmental Research Letters 7:015503.

Bradshaw, C. J. A., and I. G. Warkentin. 2015. Global estimates of boreal forest carbon stocks and flux. Global and Planetary Change 128:24–30.

Brown, J. H., O. J. Ferrians Jr., J. A. Heginbottom, and E. S. Melnikov. 1998. Circum-arctic map of permafrost and ground ice conditions. National Snow and Ice Data Center, Digital Media, Boulder, Colorado, USA.

CAVM Team. 2003. Circumpolar arctic vegetation map. (1:7,500,000 scale), Conservation of Arctic Flora and Fauna (CAFF) Map No. 1. U.S. Fish and Wildlife Service, Anchorage, Alaska, USA.

Chapin III, F. S., G. R. Shaver, A. E. Giblin, K. J. Nadelhoffer, and J. A. Laundre. 1995. Responses of arctic tundra to experimental and observed changes in climate. Ecology 76:694–711.

Chapin III, F. S., M. D. Robards, H. P. Huntington, J. E. Johnstone, S. E. Trainor, G. P. Kofinas, R. W. Ruess, N. Fresco, D. C. Natcher, and R. L. Naylor. 2006. Directional changes in ecological communities and social-ecological systems: A framework for prediction based on Alaskan examples. American Naturalist 168:S36–S49.

Clein, J. S., A. D. McGuire, X. Zhang, D. W. Kicklighter, J. M. Melillo, S. C. Wofsy, P. G. Jarvis, and J. M. Massheder. 2002. Historical and projected carbon balance of mature black spruce ecosystems across North America: the role of carbon-nitrogen interactions. Plant and Soil 242:15–32.

Cole, E. C., T. A. Hanley, and M. Newton. 2010. Influence of precommercial thinning on understory vegetation of young-growth Sitka spruce forests in southeastern Alaska. Canadian Journal of Forest Research 40:619–628.

D'Amore, D. V., J. D. Fellman, R. T. Edwards, E. Hood, and C. L. Ping. 2012. Hydropedology of the North American coastal temperate rainforest. Pages 351–380 *in* H. Lin, editor. Hydropedology; synergystic integration of soil science and hydrology. Academic Press, Waltham, Massachusetts, USA.

De Groot, W. J., M. D. Flannigan, and A. S. Cantin. 2013. Climate change impacts on future boreal fire regimes. Forest Ecology and Management 294:35–44.

Deal, R. L., and J. C. Tappeiner. 2002. The effects of partial cutting on stand structure and growth of western hemlock–Sitka spruce stands in southeast Alaska. Forest Ecology and Management 159:173–186.

Epstein, H. E., D. A. Walker, M. K. Raynolds, G. J. Jia, and A. M. Kelley. 2008. Phytomass patterns across a temperature gradient of the North American arctic tundra. Journal of Geophysical Research—Biogeosciences 113:2156–2202.

Euskirchen, E. S., et al. 2006. Importance of recent shifts in soil thermal dynamics on growing season length, productivity, and carbon sequestration in terrestrial high-latitude ecosystems. Global Change Biology 12:731–750.

Euskirchen, E. S., A. D. McGuire, and F. S. Chapin III. 2007. Energy feedbacks of northern high-latitude ecosystems to the climate system due to reduced snow cover during 20th century warming. Global Change Biology 13:2425–2438.

Euskirchen, E. S., A. D. McGuire, F. S. Chapin III, and T. S. Rupp. 2010. The changing effects of Alaska's boreal forests on the climate system. Canadian Journal of Forest Research 40:1336–1346.

Euskirchen, E. S., A. D. McGuire, F. S. Chapin III, S. Yi, and C. C. Thompson. 2009. Changes in vegetation in northern Alaska under scenarios of climate change, 2003–2100: implications for climate feedbacks. Ecological Applications 19: 1022–1043.

Euskirchen, E. S., M. S. Bret-Harte, G. J. Scott, C. Edgar, and G. R. Shaver. 2012. Seasonal patterns of carbon dioxide and water fluxes in three representative tundra ecosystems in northern Alaska. Ecosphere 3:1–19.

Euskirchen, E. S., A. P. Bennett, A. L. Breen, H. Genet, M. A. Lindgren, T. A. Kurkowski, A. D. McGuire, and T. S. Rupp. 2016. Consequences of changes in vegetation and snow cover for climate feedbacks in Alaska and northwest Canada. Environmental Research Letters 11:105003.

Fisher, J. B., et al. 2014. Carbon cycle uncertainty in the Alaskan Arctic. Biogeosciences 11:4271–4288.

Forster. 2007. Climate change 2007 : The physical science basis : contribution of working Group I to the Fourth Assessment Report of the Intergovernmental Panel on Climate Change. Cambridge University Press, Cambridge, New York, USA.

French, N. H. F., E. S. Kasischke, and D. G. Williams. 2002. Variability in the emission of carbon-based trace gases from wildfire in the Alaskan boreal forest. Journal of Geophysical Research—Atmospheres 107(D1). https://doi.org/10.1029/2001jd000480

Genet, H., et al. 2013. Modeling the effects of fire severity and climate warming on active layer thickness and soil carbon storage of black spruce forests across the landscape in interior Alaska. Environmental Research Letters 8:045016.

Genet, H., Y. He, A. D. McGuire, Q. Zhuang, Y. Zhang, F. Biles, D. V. D'Amore, K. Zhou, and K. D. Johnson. 2016. Terrestrial carbon modeling: baseline and projections in upland ecosystems. Pages 105–132 *in* Z. Zhu and A. D. McGuire, editors. Baseline and projected future carbon storage and greenhouse-gas fluxes in ecosystems of Alaska. U.S. Geological Survey, Reston, VA.

Goetz, S. J., M. C. Mack, K. R. Gurney, J. T. Randerson, and R. A. Houghton. 2007. Ecosystem responses to recent climate change and fire disturbance at northern high latitudes: observations and model results contrasting northern Eurasia and North America. Environmental Research Letters 2:1–9.

Gough, L., J. C. Moore, G. R. Shaver, R. T. Simpson, and D. R. Johnson. 2012. Above- and belowground responses of arctic tundra ecosystems to altered soil nutrients and mammalian herbivory. Ecology 93:1683–1694.

Goulden, M. L., A. M. S. McMillan, G. C. Winston, A. V. Rocha, K. L. Manies, J. W. Harden, and B. P. Bond-Lamberty. 2011. Patterns of NPP, GPP, respiration, and NEP during boreal forest succession. Global Change Biology 17:855–871.

Groisman, P. Y., T. R. Karl, R. W. Knight, and G. L. Stenchikov. 1994. Changes of snow cover, temperature and radiative heat-balance over the northern-hemisphere. Journal of Climate 7:1633–1656.

Grosse, G., et al. 2011. Vulnerability of high-latitude soil organic carbon in North America to disturbance. Journal of Geophysical Research—Biogeosciences 116:1–23.

Gustine, D. D., T. J. Brinkman, M. A. Lindgren, J. I. Schmidt, T. S. Rupp, and L. G. Adams. 2014. Climate-driven effects of fire on winter habitat for caribou in the Alaskan-Yukon Arctic. PLoS ONE 9:e100588.

Harden, J. W., R. K. Mark, E. T. Sundquist, and R. F. Stallard. 1992. Dynamics of soil carbon during deglaciation of the Laurentide ice sheet. Science 258:1921–1924.

Harden, J. W., K. L. Manies, M. R. Turetsky, and J. C. Neff. 2006. Effects of wildfire and permafrost on soil organic matter and soil climate in interior Alaska. Global Change Biology 12:2391–2403.

Harden, J. W., et al. 2012*a*. Field information links permafrost carbon to physical vulnerabilities of thawing. Geophysical Research Letters 39:L15704.

Harden, J. W., K. L. Manies, J. O'Donnell, K. Johnson, S. Frolking, and Z. Fan. 2012*b*. Spatiotemporal analysis of black spruce forest soils and implications for the fate of C. Journal of Geophysical Research—Biogeosciences 117:1–9.

Harris, I., P. D. Jones, T. J. Osborn, and D. H. Lister. 2014. Updated high-resolution grids of monthly climatic observations – the CRU TS3.10 dataset. International Journal of Climatology 34:623–642.

Hayes, D. J., A. D. McGuire, D. W. Kicklighter, K. R. Gurney, T. J. Burnside, and J. M. Melillo. 2011. Is the northern high latitude land-based CO_2 sink weakening? Global Biogeochemical Cycles 25:GB3018.

Hayes, D. J., D. W. Kicklighter, A. D. McGuire, M. Chen, Q. Zhuang, F. Yuan, J. M. Melillo, and S. D. Wullschleger. 2014. The impacts of recent permafrost thaw on land-atmosphere greenhouse gas exchange. Environmental Research Letters 9:045005.

Hinzman, L. D., C. J. Deal, A. D. McGuire, S. H. Mernild, I. V. Polyakov, and J. E. Walsh. 2013. Trajectory of the Arctic as an integrated system. Ecological Applications 23:1837–1868.

Hofmann, K., H. Pauli, N. Praeg, A. O. Wagner, and P. Illmer. 2016. Methane-cycling microorganisms in soils of a high-alpine altitudinal gradient. Fems Microbiology Ecology 92: fiw009.

Howard, J. O., and T. S. Setzer. 1989. Logging residue in southeast Alaska. Res. Pap. PNW-RP-405. U.S. Department of Agriculture, Forest Service, Pacific Northwest Research Station, Portland, Oregon, USA. 36 p 405. https://doi.org/10.2737/PNW-RP-405

Hugelius, G., C. Tarnocai, G. Broll, J. G. Canadell, P. Kuhry, and D. K. Swanson. 2013. The Northern Circumpolar Soil Carbon Database: spatially distributed datasets of soil coverage and soil carbon storage in the northern permafrost regions. Earth System Science Data 5:3–13.

Hugelius, G., et al. 2014. Estimated stocks of circumpolar permafrost carbon with quantified uncertainty ranges and identified data gaps. Biogeosciences 11:6573–6593.

Jafarov, E. E., V. E. Romanovsky, H. Genet, A. D. McGuire, and S. S. Marchenko. 2013. The effects of fire on the thermal stability of permafrost in lowland and upland black spruce forests of interior Alaska in a changing climate. Environmental Research Letters 8:035030.

Jensen, A. E., K. A. Lohse, B. T. Crosby, and C. I. Mora. 2014. Variations in soil carbon dioxide efflux across a thaw slump chronosequence in northwestern Alaska. Environmental Research Letters 9: https://doi.org/10.1088/1748-9326/9/2/025001

Johnson, K. D., et al. 2011. Soil carbon distribution in Alaska in relation to soil-forming factors. Geoderma 167–68:71–84.

Johnson, K. D., J. W. Harden, A. D. McGuire, M. Clark, F. Yuan, and A. O. Finley. 2013. Permafrost and organic layer interactions over a climate gradient in a discontinuous permafrost zone. Environmental Research Letters 8:035028.

Johnstone, J. F., F. S. Chapin III, T. N. Hollingsworth, M. C. Mack, V. Romanovsky, and M. Turetsky. 2010*a*. Fire, climate change, and forest resilience in interior Alaska. Canadian Journal of Forest Research 40:1302–1312.

Johnstone, J. F., T. N. Hollingsworth, F. S. Chapin, and M. C. Mack. 2010*b*. Changes in fire regime break the legacy lock on successional trajectories in Alaskan boreal forest. Global Change Biology 16:1281–1295.

Johnstone, J. F., T. S. Rupp, M. Olson, and D. Verbyla. 2011. Modeling impacts of fire severity on successional trajectories and future fire behavior in Alaskan boreal forests. Landscape Ecology 26:487–500.

Jones, B. M., G. Grosse, C. D. Arp, E. Miller, L. Liu, D. J. Hayes, and C. F. Larsen. 2015. Recent Arctic tundra fire initiates widespread thermokarst development. Scientific Reports 5:15865. https://doi.org/10.1038/srep15865

Jorgenson, M. T., C. H. Racine, J. C. Walters, and T. E. Osterkamp. 2001. Permafrost degradation and ecological changes associated with a warming climate in central Alaska. Climatic Change 48:551–579.

Kasischke, E. S., and M. R. Turetsky. 2006. Recent changes in the fire regime across the North American boreal region – Spatial and temporal patterns of burning across Canada and Alaska. Geophysical Research Letters 33:1–5.

Kasischke, E. S., D. Williams, and D. Barry. 2002. Analysis of the patterns of large fires in the boreal forest region of Alaska. International Journal of Wildland Fire 11:131–144.

Kasischke, E. S., D. L. Verbyla, T. S. Rupp, A. D. McGuire, K. A. Murphy, R. Jandt, J. L. Barnes, E. E. Hoy, P. A. Duffy, M. Calef, and M. R. Turetsky. 2010. Alaska's changing fire regime - implications for the vulnerability of its boreal forests. Canadian Journal of Forest Research-Revue Canadienne De Recherche Forestiere 40:1313–1324. https://doi.org/10.1139/x10-098

Kicklighter, D. W., D. J. Hayes, J. W. Mcclelland, B. J. Peterson, A. D. McGuire, and J. M. Melillo. 2013. Insights and issues with simulating terrestrial DOC loading of Arctic river networks. Ecological Applications 23:1817–1836.

Koven, C. D., et al. 2015. A simplified, data-constrained approach to estimate the permafrost carbon–climate feedback. Philosophical Transactions of the Royal Society A 373:20140423.

Landscape Conservation Cooperatives. 2012. Frequently asked questions. Conservation in action. U.S. Fish & Wildlife Service, Washington D.C., 4pp.

Lara, M. J., H. Genet, A. D. McGuire, E. S. Euskirchen, Y. Zhang, D. R. N. Brown, M. T. Jorgenson, V. Romanovsky, A. Breen, and W. R. Bolton. 2016. Thermokarst rates intensify due to climate change and forest fragmentation in an Alaskan boreal forest lowland. Global Change Biology 22:816–829.

Liljedahl, A. K., et al. 2016. Pan-Arctic ice-wedge degradation in warming permafrost and its influence on tundra hydrology. Nature Geoscience 9:312–318.

Luo, Y., et al. 2016. Toward more realistic projections of soil carbon dynamics by earth system models. Global Biogeochemical Cycles 30:40–56. https://doi.org/10.1002/2015GB005239

Lyu, Z., Y. He, H. Genet, A. D. McGuire, Q. Zhuang, B. Wylie, and Y. Zhang. 2016. Wetland carbon dynamics in Alaska from 1950 to 2099. Pages 133–158 *in* Z. Zhu and A. D. McGuire, editors. Baseline and projected future carbon storage and greenhouse-gas fluxes in ecosystems of Alaska. U.S. Geological Survey, Reston, VA.

Mack, M. C., M. S. Bret-Harte, T. N. Hollingsworth, R. R. Jandt, E. A. G. Schuur, G. R. Shaver, and D. L. Verbyla. 2011. Carbon loss from an unprecedented Arctic tundra wildfire. Nature 475:489–492.

Malone, T., J. Liang, and C. Packee. 2009. Cooperative Alaska forest inventory. Page 42. Gen. Tech. Rep. PNW-GTR-785, U.S. Department of Agriculture, Portland, Oregon, USA.

Mann, D. H., T. S. Rupp, M. A. Olson, and P. A. Duffy. 2012. Is Alaska's boreal forest now crossing a major ecological threshold? Arctic Antarctic and Alpine Research 44:319–331.

Martineau, C., L. G. Whyte, and C. W. Greer. 2010. Stable isotope probing analysis of the diversity and activity of methanotrophic bacteria in soils from the Canadian high arctic. Applied and Environmental Microbiology 76:5773–5784.

McFarlane, N. A., G. J. Boer, J.-P. Blanchet, and M. Lazare. 1992. The Canadian climate centre second-generation general circulation model and its equilibrium climate. Journal of Climate 5:1013–1044.

McGuire, A. D., J. M. Melillo, L. A. Joyce, D. W. Kicklighter, A. L. Grace, B. Moore III, and C. J. Vorosmarty. 1992. Interactions between carbon and nitrogen dynamics in estimating net primary productivity for potential vegetation in North America. Global Biogeochemical Cycles 6:101–124.

McGuire, A. D., et al. 2010. An analysis of the carbon balance of the Arctic Basin from 1997 to 2006. Tellus 62B:455–474.

McGuire, A. D., et al. 2012. An assessment of the carbon balance of Arctic tundra: comparisons among observations, process models, and atmospheric inversions. Biogeosciences 9:3185–3204.

McGuire, A. D., et al. 2016. Variability in the sensitivity among model simulations of permafrost and carbon dynamics in the permafrost region between 1960 and 2009. Global Biogeochemical Cycles 30:1015–1037.

Melvin, A. M., M. C. Mack, J. F. Johnstone, A. D. McGuire, H. Genet, and E. A. G. Schuur. 2015. Differences in ecosystem carbon distribution and nutrient cycling linked to forest tree species composition in a mid-successional boreal forest. Ecosystems 18:1472–1488.

Michaelson, G. J., C. L. Ping, and M. H. Clark. 2013. Soil pedon carbon and nitrogen data for Alaska: An analysis and update. Open Journal of Soil Science 3:132–142.

Moosavi, S. C., and P. M. Crill. 1997. Controls on CH_4 and CO_2 emissions along two moisture gradients in the Canadian boreal zone. Journal of Geophysical Research—Atmospheres 102:29261–29277.

Myers-Smith, I. H., et al. 2011. Shrub expansion in tundra ecosystems: dynamics, impacts and research priorities. Environmental Research Letters 6:045509.

Nakicenovic, N., et al. 2000. Special report on emissions scenarios. Cambridge University Press, Cambridge, UK, 597pp.

North American Land Change Monitoring System. 2005. North American land cover at 250 m spatial resolution (edition 1.0): Natural Resources Canada/Canadian Center for Remote Sensing (NRCan/CCRS), United States GeologicalSurvey (USGS); Insituto Nacional de Estadística y Geografía (INEGI), Comisión Nacional para el Conocimiento y Uso de la Biodiversidad (CONABIO), and Comisión NacionalForestal (CONAFOR). http://www.cec.org/tools-and-resources/map-files/land-cover-2005

Nitze, I., and G. Grosse. 2016. Detection of landscape dynamics in the Arctic Lena Delta with temporally dense Landsat time-series stacks. Remote Sensing of Environment 181:27–41.

Norby, R. J., et al. 2005. Forest response to elevated CO_2 is conserved across a broad range of productivity. Proceedings of the National Academy of Sciences USA 102:18052–18056.

Nowacki, G., P. Spencer, M. Fleming, T. Brock, and T. M. Jorgenson. 2001. Unified Ecoregions of Alaska: 2001. U.S. Geological Survey Open-File Report 2002-297 (map). U.S. Geological Survey, Reston, VA.

Olefeldt, D., et al. 2016. Circumpolar distribution and carbon storage of thermokarst landscapes. Nature Communications 7:13043.

Parent, M. B., and D. Verbyla. 2010. The browning of Alaska's boreal forest. Remote Sensing 2:2729–2747.

Pastick, N. J., et al. 2017. Historical and projected trends in landscape drivers affecting carbon dynamics in Alaska. Ecological Applications 27:1383–1402. https://doi.org/10.1002/eap.1538

Piao, S., et al. 2013. Evaluation of terrestrial carbon cycle models for their response to climate variability and to CO_2 trends. Global Change Biology 19:2117–2132.

Raich, J. W., E. B. Rastetter, J. M. Melillo, D. W. Kicklighter, P. A. Steudler, B. J. Peterson, A. L. Grace, B. Moore, and C. J. Vorosmarty. 1991. Potential net primary productivity in South-America – application of a global-model. Ecological Applications 1:399–429.

Rastetter, E. B., A. W. King, B. J. Cosby, G. M. Hornberger, R. V. Oneill, and J. E. Hobbie. 1992. Aggregating fine-scale ecological knowledge to model coarser-scale attributes of ecosystems. Ecological Applications 2:55–70.

Roeckner, E., R. Brokopf, M. Esch, M. Giorgetta, S. Hagemann, L. Kornblueh, E. Manzini, U. Schlese, and U. Schulzweida. 2004. The atmospheric general circulation model ECHAM5 Part II: Sensitivity of simulated climate to horizontal and vertical resolution. Max Planck Institut für Meteorologie, Hamburg, Germany.

Romanovsky, V. E., et al. 2010. Thermal state of permafrost in Russia. Permafrost and Periglacial Processes 21:136–155.

Ruess, R. W., K. VanCleve, J. Yarie, and L. A. Viereck. 1996. Contributions of fine root production and turnover to the carbon and nitrogen cycling in taiga forests of the Alaskan interior. Canadian Journal of Forest Research 26:1326–1336.

Rupp, T. S., F. S. Chapin, and A. M. Starfield. 2001. Modeling the influence of topographic barriers on treeline advance at the forest-tundra ecotone in northwestern Alaska. Climatic Change 48:399–416.

Rupp, T. S., A. M. Starfield, F. S. Chapin, and P. Duffy. 2002. Modeling the impact of black spruce on the fire regime of Alaskan boreal forest. Climatic Change 55:213–233.

Rupp, T. S., X. Chen, M. Olson, and A. D. McGuire. 2007. Sensitivity of simulated boreal fire dynamics to uncertainties in climate drivers. Earth Interactions 11:1–21.

Rupp, T. S., P. Duffy, M. Leonawicz, M. A. Lindgren, A. L. Breen, T. Kurkowski, A. Floyd, A. Bennett, and L. Krutikov. 2016. Climate simulations, land cover, and wildfire. Pages 17–52 *in* Z. Zhu and A. D. McGuire, editors. Baseline and projected future carbon storage and greenhouse-gas fluxes in ecosystems of Alaska. U.S. Geological Survey, Reston, VA.

Schuur, E. A. G., et al. 2008. Vulnerability of permafrost carbon to climate change: Implications for the global carbon cycle. BioScience 58:701–714.

Schuur, E. A. G., J. G. Vogel, K. G. Crummer, H. Lee, J. O. Sickman, and T. E. Osterkamp. 2009. The effect of permafrost thaw on old carbon release and net carbon exchange from tundra. Nature Letters 459: https://doi.org/10.1038/nature08031

Schuur, E. A. G., et al. 2015. Climate change and the permafrost carbon feedback. Nature 520:171–179.

Shaver, G. R., and F. S. Chapin III. 1991. Production: Biomass relationships and element cycling in contrasting arctic vegetation types. Ecological Monographs 61:1–31.

Sistla, S. A., J. C. Moore, R. T. Simpson, L. Gough, G. R. Shaver, and J. P. Schimel. 2013. Long-term warming restructures Arctic tundra without changing net soil carbon storage. Nature 497:615–618.

Sitch, S., A. D. McGuire, J. Kimball, N. Gedney, J. Gamon, R. Engstrom, A. Wolf, Q. Zhuang, J. Clein, and K. C. McDonald. 2007. Assessing the carbon balance of circumpolar Arctic tundra using remote sensing and process modeling. Ecological Applications 17:213–234.

Stackpoole, S. M., D. E. Butman, D. W. Clow, K. L. Verdin, B. V. Gaglioti, H. Genet, and R. Striegl. 2017. Inland waters and their role in the carbon cycle of Alaska. Ecological Applications 27:1403–1420.

Stow, D. A., et al. 2004. Remote sensing of vegetation and land-cover change in Arctic tundra ecosystems. Remote Sensing of Environment 89:281–308.

Sturm, M., C. Racine, and K. Tape. 2001. Climate change—increasing shrub abundance in the Arctic. Nature 411:546–547.

Sullivan, P. F., M. Sommerkorn, H. M. Rueth, K. J. Nadelhoffer, G. R. Shaver, and J. M. Welker. 2007. Climate and species affect fine root production with long-term fertilization in acidic tussock tundra near Toolik Lake, Alaska. Oecologia 153:643–652.

Tape, K., M. Sturm, and C. Racine. 2006. The evidence for shrub expansion in Northern Alaska and the Pan-Arctic. Global Change Biology 12:686–702.

Turetsky, M. R., E. S. Kane, J. W. Harden, R. D. Ottmar, K. L. Manies, E. Hoy, and E. S. Kasischke. 2011. Recent acceleration of biomass burning and carbon losses in Alaskan forests and peatlands. Nature Geoscience 4:27–31.

Van Wijk, M. T., M. Williams, J. A. Laundre, and G. R. Shaver. 2003. Interannual variability of plant phenology in tussock tundra: modelling interactions of plant productivity, plant phenology, snowmelt and soil thaw. Global Change Biology 9:743–758.

Verbyla, D. 2011. Browning boreal forests of western North America. Environmental Research Letters 6:1–3.

Walker, X., and J. F. Johnstone. 2014. Widespread negative correlations between black spruce growth and temperature across topographic moisture gradients in the boreal forest. Environmental Research Letters 9:064016.

Walter, B. P., and M. Heimann. 2000. A process-based, climate-sensitive model to derive methane emissions from natural wetlands: Application to five wetland sites, sensitivity to model parameters, and climate. Global Biogeochemical Cycles 14:745–765.

Whalen, S., and W. Reeburgh. 1990. Consumption of atmospheric methane by tundra soils. Nature 346:160–162.

Whittaker, R. H. 1975. Communities and ecosystems. Macmillan, New York, New York, USA.

Woo, M.-K., M. A. Arain, M. Mollinga, and S. Yi. 2004. A two-directional freeze and thaw algorithm for hydrologic and land surface modelling. Geophysical Research Letters 31: L12501.

Yi, S., M. A. Arain, and M.-K. Woo. 2006. Modifications of a land surface scheme for improved simulation of ground freeze-thaw in northern environments. Geophysical Research Letters 33:L13501.

Yi, S., K. Manies, J. Harden, and A. D. McGuire. 2009*a*. Characteristics of organic soil in black spruce forests: Implications for the application of land surface and ecosystem models in cold regions. Geophysical Research Letters 36:L05501.

Yi, S., et al. 2009*b*. Interactions between soil thermal and hydrological dynamics in the response of Alaska ecosystems to fire disturbance. Journal of Geophysical Research—Biogeosciences 114:G02015.

Yi, S., A. D. McGuire, E. Kasischke, J. Harden, K. Manies, M. Mack, and M. Turetsky. 2010. A dynamic organic soil biogeochemical model for simulating the effects of wildfire on soil environmental conditions and carbon dynamics of black spruce forests. Journal of Geophysical Research—Biogeosciences 115: G04015.

Yuan, F. M., S. H. Yi, A. D. McGuire, K. D. Johnson, J. Liang, J. W. Harden, E. S. Kasischke, and W. A. Kurz. 2012. Assessment of boreal forest historical C dynamics in the Yukon River Basin: relative roles of warming and fire regime change. Ecological Applications 22:2091–2109.

Zeng, H., G. Jia, and H. Epstein. 2011. Recent changes in phenology over the northern high latitudes detected from multi-satellite data. Environmental Research Letters 6:045508.

Zhou, X., S. A. Schroder, A. D. McGuire, and Z. Zhu. 2016. Chapter 5. Forest inventory-based analysis and projections of forest carbon stocks and changes in Alaskan coastal forests. Pages 95–104 *in* Z. Zhu and A. D. McGuire, editors. Baseline and projected future carbon storage and greenhouse-gas fluxes in ecosystems of Alaska. U.S. Geological Survey Professional Paper 1826, Reston, VA.

Zhuang, Q., A. D. McGuire, K. P. O'Neill, J. W. Harden, V. E. Romanovsky, and J. Yarie. 2002. Modeling soil thermal and carbon dynamics of a fire chronosequence in interior Alaska. Journal of Geophysical Research—Atmospheres 108:1–25.

Zhuang, Q., et al. 2003. Carbon cycling in extratropical terrestrial ecosystems of the northern hemisphere during the 20th century: a modeling analysis of the influences of soil thermal dynamics. Tellus Series B: Chemical and Physical Meteorology 55:751–776.

Zhuang, Q., J. M. Melillo, D. W. Kicklighter, R. G. Prinn, A. D. McGuire, P. A. Steudler, B. S. Felzer, and S. Hu. 2004. Methane fluxes between terrestrial ecosystems and the atmosphere at northern high latitudes during the past century: A retrospective analysis with a process-based biogeochemistry model. Global Biogeochemical Cycles 18:GB3010.

Zhuang, Q., M. Chen, K. Xu, J. Tang, E. Saikawa, Y. Lu, J. M. Melillo, R. G. Prinn, and A. D. McGuire. 2013. Response of global soil consumption of atmospheric methane to changes in atmospheric climate and nitrogen deposition. Global Biogeochemical Cycles 27: https://doi.org/10.1002/gbc.20057

Supporting Information

Additional supporting information may be found online at: http://onlinelibrary.wiley.com/doi/10.1002/eap.1641/full

Data Availability

Data available from the Scenario Network for Alaska Planning data portal and the USGS Science Base. Scenario Network for Alaska Planning data portal: https://doi.org/10.5066/f7td9w8z. USGS Science Base: https://www.sciencebase.gov/catalog/item/59a40544e4b077f005673247.